Reduce, Reuse, Recycle: The tale of two Wnts and the lone *C. elegans* Syndecan, SDN-1

BY

Samantha N. Hartin

Submitted to the graduate degree program in Molecular Biosciences and the Graduate Faculty of the University of Kansas in partial fulfillment of the requirements for the degree of Doctor of Philosophy.

_____
Chairperson – Dr. Brian D. Ackley

_____
Dr. Erik Lundquist

_____
Dr. Stuart Macdonald

_____
Dr. Robert Ward

_____
Dr. Yoshiaki Azuma

_____
Dr. Elias Michaelis

Date defended: May 1, 2015

The dissertation committee for Samantha N. Hartin
certifies that this is the approved version of the following dissertation:

Reduce, Reuse, Recycle: The tale of two Wnts and the lone *C. elegans* Syndecan, SDN-1

_____
Chairperson – Dr. Brian D. Ackley

Date approved: May 1, 2015

Abstract

Heparan sulfate proteoglycans (HSPGs) are cell adhesion molecules that have been shown to be involved in a myriad of different aspects of development such as embryogenesis, dorsal-ventral axon guidance and cell migration. Despite knowing the phenotypes caused by mutations in HSPGs, little is known about the ligands working with HSPGs during development. Identification of HSPG ligands will provide insight into how HSGPs function during embryogenesis and later in neural development.

Chapter II describes two *Caenorhabditis elegans* cell adhesion proteins SDN-1/Syndecan and PTP-3/LAR-RPTP as important regulators of polarization and cell migration during embryogenesis. Loss-of-function (LOF) mutations in either *ptp-3* or *sdn-1* resulted in low penetrance embryonic developmental defects. We used double mutant analysis to test whether *ptp-3* and *sdn-1* function in a linear genetic pathway during *C. elegans* embryogenesis and found that double mutants of *sdn-1* and *ptp-3* exhibited a highly penetrant synthetic lethality (SynLet), with only a small percentage of animals surviving to adulthood. Analysis of the survivors demonstrated that these animals had a synergistic increase in the penetrance of embryonic developmental defects. Taken together, these data strongly suggested that PTP-3 and SDN-1 function in parallel during embryogenesis. We subsequently used RNAi to knockdown the function of ~3,600 genes predicted to encode secreted and/or transmembrane molecules to identify genes that interacted with *ptp-3* or *sdn-1*. We found that the Wnt ligand, *lin-44,* was SynLet with *sdn-1* but not *ptp-3.* We used 4-dimensional time-lapse analysis to characterize the interaction between *lin-44* and *sdn-1*. We found evidence that loss of *lin-44* caused defects in the polarization

and migration of endodermal precursors during gastrulation, a previously undescribed role for *lin-44* that is strongly enhanced by the loss of *sdn-1*.

In chapter III the interaction between SDN-1, LIN-44 and EGL-20 during DD/VD (Dorsal D-type and Ventral D-type motorneurons, respectively) axon outgrowth and termination is described. Double mutant analysis between *sdn-1, lin-44* and *egl-20* suggests SDN-1 acts extrinsically to inhibit the activation of BAR-1/β-catenin during axon outgrowth of the D-type motorneurons specifically, DD6 and VD13. Then SDN-1 acts intrinsically within the Wnt signaling pathway to ensure proper outgrowth termination of those axons. These results show for the first time that the same Wnt signaling pathways are both positively and negatively regulated by SDN-1 during axon growth.

Altogether, our genetic analysis suggest that axon outgrowth and termination occurs in two steps with Wnt ligands acting with SDN-1 in a combinatorial fashion and are not simply working in a parallel manner as previously reported.

Acknowledgements

First, I would like to thank my parents for their constant love and encouragement. Despite not coming from science backgrounds both my parents took an active role in learning about my studies. My father went so far as to look up videos of key note speakers from the conferences I attended. Both always made sure to tell everyone that their baby girl was getting her PhD! Their pride and complete faith in me, always served to boost my spirits when I was overwhelmed. To my parents, Steve and Sandy, I love you and thank you so much. To my older brother Brett, I win! To Anthony, thank you for being there through undergraduate and graduate school.

I would like to thank my mentor, Dr. Brian Ackley. Thank you for putting up with me for six and a half years. You let me be my best and sometimes not so best self in lab. I consider myself lucky to have been able to join your lab and grow as a scientist under your tutelage. You even trusted me enough to pass my knowledge and skills on to undergraduate researchers. I also want to thank Dr. Martin Hudson for his invaluable contributions to the embryogenesis work.

I would also like to thank members of the Ackley and Lundquist lab for all their help, input, support, and friendship during my graduate school experience. Especially Dr. Erik Lundquist for his advice and insight during our joint lab meetings.

Finally, I'd like to thank Angie Fowler and Lakshmi Sundararajan, two friends that have been there since the beginning. To my lab mate, Vi Leitenberger, thank you for your friendship, support, endless supply of gossip and shenanigans throughout graduate school.

Table of Contents

Page number

List of Figures

Figure **Page number**

List of Tables

Table **Page number**

Chapter I
Introduction

Predictions indicate that around 20-30% of the human genome encodes for proteins that are present in the extracellular matrix (ECM) [1, 2]. Predictions for other organisms are similar, suggesting that these numbers are accurate [3, 4]. Understanding how the proteins present in the ECM function during development in a spatio-temporal manner is vital to understanding how these same molecules can contribute to different developmental diseases such as, osteogenesis imperfecta, Ehlers-Danlos Syndromes, Marfan syndrome, fibrosis, chondrodysplasias and some cancers [5].

Secreted and transmembrane molecules have multiple roles in the development and maintenance of all cell types. Proteins present in the ECM provide adhesion and support as well as positional and instructional cues to cells throughout development, particularly during nervous system development. Through the ECM and particularly with the help of cell adhesion molecules, cells are able to gather and respond to extracellular cues that are critical for cell differentiation and migration. During nervous system development, when a neuron has migrated to the correct position it must then respond to more instructional cues in order to extend an axon to the proper location and form a synapse. The dynamics of the ECM are tightly regulated to ensure proper development. Abnormal ECM dynamics can lead to improper cell processes that can in turn lead to disease [5].

The ECM is a heterogeneous network that allows for cellular communication and is comprised of interlocking fibrous proteins and glycoproteins. The basal lamina, or basement membrane of the ECM is of particular importance because it provides an attachment substrate for cells during development. The composition of

the basal lamina varies upon developmental timing and location, but it is mainly composed of laminins, collagens, nidogens and heparan sulfate proteoglycans (HSPGs) [2]. These proteins not only provide trophic support and adhesion but positional and instructional cues as well.

Cell adhesion molecules (CAMs) provide multiple functions during the development and homeostasis of an organism.

Research on molecules present in the ECM has identified cell adhesion molecules as a class of proteins that are needed for multiple critical aspects of development [6]. Cell adhesion proteins allow cells to communicate with one another and their surrounding environment. They control the complex signaling pathways in which alterations can lead to substantial changes in cell behavior including division, differentiation and migration.

LAR/PTP-3 and syndecan/SDN-1 [7-9], among others, have been identified to contribute during embryonic development and later to neural development. LAR/PTP-3 is a member of the type IIa family of tyrosine phosphatases [10]. LAR family members, including *C. elegans* PTP- 3, are involved in epidermal closure, axon guidance and synaptogenesis [9, 11-14]. Additionally, the cell-surface associated HSPGs, syndecans have been implicated in a broad range of developmental events such as, epidermal closure, ventral neuroblast migration, axon guidance and neuron migration [15-17]. In this work I will discuss our findings regarding the interaction of *ptp-3* and *sdn-1* during embryogenesis and how their synthetic lethal (SynLet)

relationship can help to identify other potential genes involved in embryonic development.

We found that *ptp-3* and *sdn-1* function in parallel signaling pathways during *C. elegans* embryogenesis. *ptp-3; sdn-1* double mutants exhibit a highly penetrant SynLet phenotype, with development arresting during embryogenesis or in the first larval stage (L1). We conducted an RNAi screen using the SynLet phenotype to identify potential *ptp-3* and *sdn-1* interactors from a library of clones encoding for molecules either attached to the membrane or secreted into the extracellular space. One candidate gene, *lin-44* displayed a strong SynLet phenotype with *sdn-1* but not *ptp-3*. Further analysis showed that *lin-44* works in the same pathway as *ptp-3* during early gastrulation events and in parallel to *sdn-1*.

LIN-44 is a member of the highly conserved Wnt family of secreted glycoproteins. Wnt signaling has been shown to be involved in neuronal migrations, cell polarity, axon guidance and synapse formation along the anterior-posterior (AP) axis, all of which are important in neural circuit assembly in *C. elegans*, *Drosophila* and mice [18-22]. Organisms that have mutations in Wnt pathways exhibit a range of developmental defects such as axis duplication, AP patterning defects, embryonic lethality, central nervous system defects, limb defects, and cancers [23, 24].

C. elegans D-type motorneurons as a model for axon outgrowth and termination

Work in Chapter III of this dissertation is centered on understanding how SDN-1 and Wnt signaling genetically interact during the outgrowth and termination

of the DD/VD motorneurons. Wnts provide both long and short range signals that contribute to the formation and patterning of complex body structures like the metazoan nervous system. As with other tissues, cells of the nervous system must be able to respond to the appropriate cues throughout development. Alterations in this developmental signaling can lead to neurological disorders and even cancer [23, 24]. Therefore, it is important to understand the signaling pathways that control the development and maintenance of the nervous system.

Like the human nervous system, the *C. elegans* nervous system consists of cells with specific segmental or tiling identity, where some neurons grow to the boundary and then terminate growth, while others grow into other segments [25-28]. This "neighborhood" hypothesis proposed by White et al., 1983 and 1986, supposes that *C. elegans* axons grow by following "neighborhood-specific surface molecules as recognition cues" [25, 29]. The conserved family of Wnt ligands contribute to the tiling of the nervous system and have been implicated in neurological disease and cancer. Wnt ligands are expressed in a gradient along the anterior-posterior (AP) axis of the *C. elegans* body and are capable of signaling through multiple receptors such as the HSPG, Syndecan, among others. In this context, Syndecans function as an activator or an inhibitor of Wnt signaling in a cell type dependent manner during vertebrate and invertebrate development [30-35]. However, in vertebrates and invertebrates we don't understand how cells of the same type are able to respond differently to extracellular cues to form the segmental pattern of the nervous system.

We utilize the green fluorescently labeled marker, *juIs76* in the model organism *C. elegans* to study the effects of disruptions in Wnt signaling and *sdn-1* function to better understand how these genes genetically interact. The *juIs76* strain contains GFP driven by the GABAergic specific promoter *unc-25*, which has been widely used as a marker for DD/VD motorneurons [36-39]. The *C. elegans* nervous system is made up of 302 neurons. Nematode nervous system development is highly conserved with the nervous system development in humans, making it an ideal model for studying neurodevelopmental disorders [25]. The same directional growth decisions (anterior-posterior and dorsal-ventral) made by neurons in the mammalian brain must also be made in *C. elegans* neural development. The D-type motorneuron cell bodies are located along the ventral nerve cord (VNC). The 6 DD neurons form during embryogenesis followed by the 13 VD neurons during the L1/L2 larval stages. These neurons innervate body wall muscles and are responsible for reciprocal inhibition during locomotion. The DD/VD neurons extend a process anteriorly, bifurcate and send a process dorsally. Once they reach the dorsal nerve cord (DNC), they bifurcate again to send a process anteriorly and posteriorly (Figure 1.1).

The work in this dissertation focuses on the development of the two most posterior DD/VD cells, DD6 and VD13 (Figure 1.1). In the dorsal nerve cord, the DD/VD axons fasciculate to form a bundle with only two axons overlapping at a time, terminating at stereotyped positions along the anterior-posterior axis. Furthermore, the DD6 and VD13 axon form a bundle in which the DD6 axon terminates at the posterior edge of the corresponding cell body on the ventral nerve

cord and the VD13 axon extends slightly farther posteriorly, terminating at the posterior edge of the VD13 cell body (Figure 1.1) [40]. Despite these data, the molecular events underpinning these stereotyped morphologies are not well understood. Because of these stereotyped neuronal tracts, the D-type motorneurons in *C. elegans* present an opportunity to study how a neuron differentially responds to the same cues for axon outgrowth and termination.

Axon outgrowth is combinatorially controlled by SDN-1 and the Wnt ligands, LIN-44 and EGL-20

As stated above, during our SynLet genetic screen we identified *lin-44* as a potential ligand for *ptp-3,* working in a parallel pathway to *sdn-1* [41]. Because of this early interaction with *lin-44* we sought to determine whether *ptp-3* or *sdn-1* interacted with *lin-44* in axon guidance.

LIN-44 is one of five Wnt ligands encoded by the *C. elegans* genome and is expressed primarily in hypodermal cells located in the tail [42-45]. Wnts are one family of secreted molecules that serve to pattern the embryo and also provide axon guidance cues in later developmental stages [46]. Loss of *lin-44* in *C. elegans* causes the DD6 and/or VD13 axons to over-extend into the posterior region of the animal (Figure 1.2) [40]. Traditionally, Wnt/LIN-44 was thought to control the transcription of target genes via canonical Wnt signaling pathway that includes Frizzled/LIN-17, Dishevelled/MIG-5, Axin/PRY-1, GSK3β/GSK-3 and β-catenin/BAR-1 (Figure 1.3). EGL-20, another posteriorly expressed Wnt ligand was previously thought to work in a redundant pathway to ensure proper axon

termination due to the synergistic phenotype seen in *lin-44;egl-20* double mutants [40]. However, in this work we show that the mechanism for axon termination is not as simple as a one-to-one parallel pathway and indeed *sdn-1* plays a pivotal role in the posterior growth and termination of the D-type motorneurons.

We found that LOF mutations in *sdn-1* caused the DD6 and/or VD13 axons to over-extend as well as under-extend. This phenotype was similar to *lin-17*/Frizzled and *mig-5*/Dishevelled, mutations in the canonical Wnt pathway [40]. Complete LOF mutations in *sdn-1* suppress the over-extension exhibited in the *lin-44* single mutants comparable to *sdn-1*. However, *lin-44;sdn-1* double mutants display under-extension defects similar to those in *sdn-1* LOF mutants. These data suggest that *sdn-1* is epistatic to *lin-44* in a genetic pathway needed for both axon outgrowth and termination.

Since *egl-20* has been shown to have a synergistic relationship with *lin-44* for axon termination we analyzed whether *sdn-1* interacts with *egl-20* [40]. EGL-20 is another Wnt ligand that is produced from hypodermal cells located anterior to where LIN-44 is expressed. EGL-20 can act as a long range and short range signal for Q neuroblast and distal tip cell migration [31, 45]. In contrast to what was previously observed in *egl-20* mutants, we found that total loss of *egl-20* causes the axons to over-extend in a higher percentage of animals than in the weak LOF allele. This difference is most likely due to the fact a weak LOF allele was used before instead of a null allele [40]. Double mutant analysis of *sdn-1* and a putative *egl-20* null allele revealed that *sdn-1* acts downstream of *egl-20* in a pathway that is

important for axon outgrowth and that they both have smaller roles in axon termination alongside LIN-44.

The side chains of SDN-1 are important for axon guidance, cell migration and early development [15, 17, 47-52]. After side chain addition by EXT enzymes, the chains are modified by an N-deactylase-N-sulfotransferase. Then an epimerase (HSE-5) and two sulfotransferases (HST-2 and HST-6) modify the sugar moieties that regulate specific receptor-ligand interactions [52, 53]. Single mutants of each gene displayed variable phenotypes similar in either under or over-extension to *sdn-1* mutants. When HS modifier genes were mutated in combination with either Wnt ligand the HS mutants did not fully recapitulate the phenotypes seen in *sdn-1;Wnt* double mutants. These suggest there may be another proteoglycan and/or modifying enzyme involved in these two processes. Further analysis will be needed to confirm this hypothesis.

Since SDN-1 is expressed in both the nervous system and surrounding tissues we sought to determine where SDN-1 is functioning during axon outgrowth and termination. We employed the use of two separate Mos-SCI (Mos1 mediated Single Copy transgene Insertion) strains, each containing a single copy of the full-length *sdn-1* gene under its endogenous promoter. Both strains were able to rescue the under-extension of the axons but not the over-extension, which may be due to missing regulatory elements. Next we used a cell specific construct to determine if SDN-1 is acting specifically in the DD/VD neurons. We found that at two separate concentrations our construct decreased the penetrance of the over-extension phenotype but not under-extension as seen with the Mos-SCI strains.

In summary, we created a screening paradigm that allows for the identification of signaling molecules that may be missed in traditional forward genetic screens. The findings from our screen allowed us to identify a novel function for LIN-44 during gastrulation. Based on our later axon guidance studies, we determined that SDN-1 and LIN-44 act together along with downstream Wnt effectors to ensure proper DD/VD axon outgrowth and termination. By using null mutations, we have revealed new insights as to how the original pathways are thought to function in these processes. Specifically, we found that LIN-44 and EGl-20 do not simply function in a one-to-one signaling pathway but function combinatorially during these two separate processes.

Section 1.1 Figures

Figure 1.1

A.

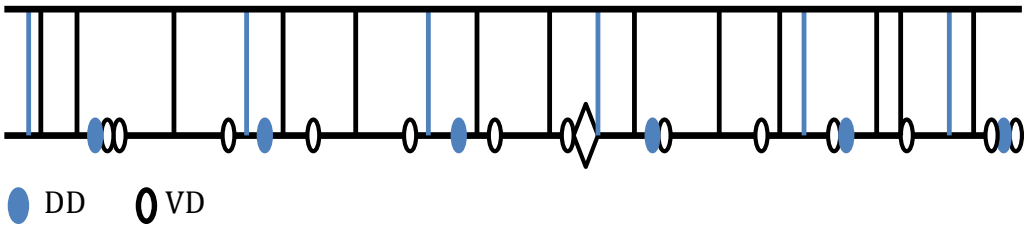

B.

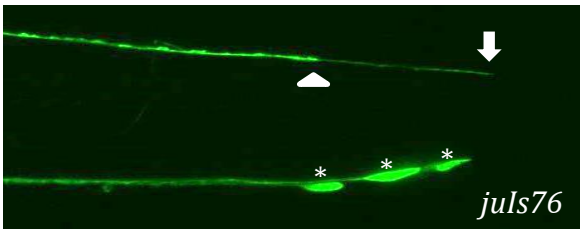

Figure 1.1 DD/VD GABAergic motorneurons grow to stereotyped positions along the anterior-posterior body axis (A) A schematic of the DD/VD motorneurons. Blue indicates the approximate location of the six DD motorneurons. White indicates the approximate location of the VD motorneurons. (B) The posterior most motorneurons, VD12, DD6 and VD13 (asterisks) are visualized with *juIs76*. The arrowhead indicates the termination of the DD6 axon in the dorsal nerve cord. The arrow indicates the stereotyped termination point for the VD13 axon at the poster edge of the cell bodies located in the ventral nerve cord.

Figure 1.2

A.

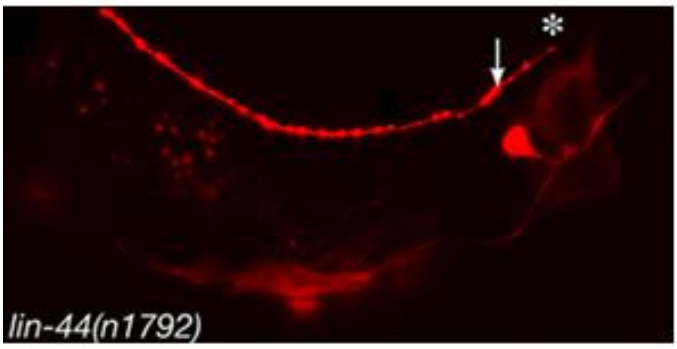

B.

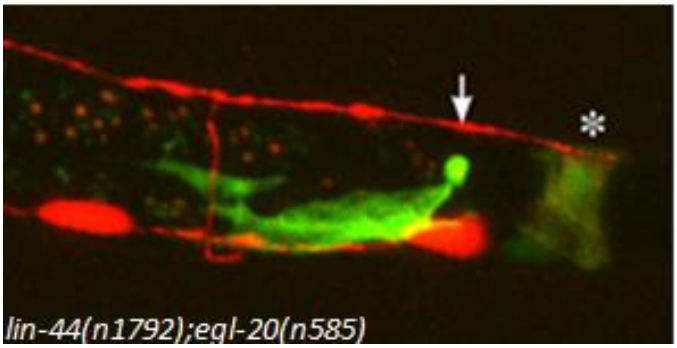

Figure 1.2 LIN-44 and EGL-20 work in parallel pathways for axon termination

(A) Over-extension defects occur in *lin-44(n1792)* and *egl-20(n585)* mutants. *The lin-44(n1792)* over-extension is quantitatively more severe than what is seen in *egl-20(n585)* (not shown). (B) *lin-44(n1792);egl-20(n585)* double mutants display the most severe over-extension defects suggesting they work in parallel for axon termination. *wyIs75* [*Punc-47*::DsRed] was used to visualize the DD/VD motorneurons. Arrow indicates stereotyped termination point. Asterisk indicates mutant termination point [40].

Figure 1.3

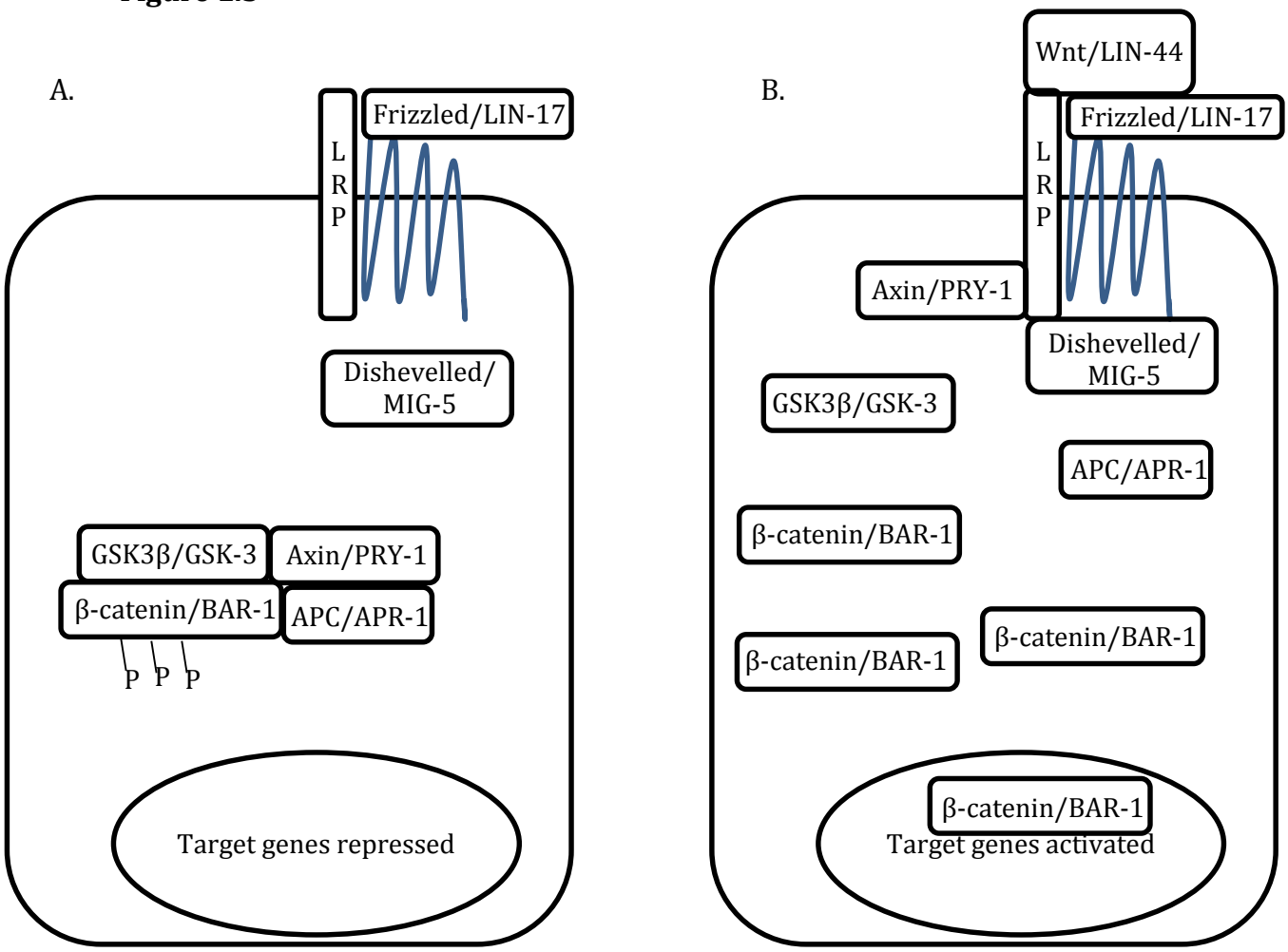
A.
Frizzled/LIN-17
L
R
P
Dishevelled/
MIG-5
GSK3β/GSK-3
Axin/PRY-1
β-catenin/BAR-1
APC/APR-1
P P P
Target genes repressed
B.
Wnt/LIN-44
Frizzled/LIN-17
L
R
P
Axin/PRY-1
Dishevelled/
MIG-5
GSK3β/GSK-3
APC/APR-1
β-catenin/BAR-1
β-catenin/BAR-1
β-catenin/BAR-1
β-catenin/BAR-1
Target genes activated

Figure 1.3 Canonical Wnt signaling pathway in *C. elegans* (A) In the absence of a Wnt ligand the Axin/APC/GSK3β complex phosphorylates β-catenin and targets it for degradation. Transcription of Wnt target genes is repressed. (B) In the presence of a Wnt ligand, the Frizzled receptor activates Dishevelled which then inhibits the Axin/APC/GSK3β complex from phosphorylating β-catenin. β-catenin then builds up in the cytoplasm and enters the nucleus to initiate the transcription of Wnt target genes.

Chapter II

A synthetic lethal screen identifies a role for *lin-44*/Wnt in *Caenorhabditis elegans* embryogenesis

Section 2.1 Abstract

Cell adhesion molecules such as the Leukocyte-common antigen related receptor, LAR/PTP-3 and the heparan sulfate proteoglycan (HSPG) syndecan, SDN-1 have been shown to be involved in multiple developmental events, including but not limited to neurogenesis in mammals, *Drosophila* and *C. elegans* [15, 16, 54-60]. Previously, we have demonstrated that the *ptp-3B* isoform is needed for cell migration and proper axon guidance, while the *ptp-3*A isoform regulates synapse formations and lacks other phenotypes associated with alleles common to all *ptp-3* isoforms.

Syndecans are short single pass transmembrane proteins with short intracellular domains. The extracellular domains are decorated with heparan sulfate and chondroitin sulfate side chains and the intracellular domain links to cytoplasmic signaling via a PDZ like motif. The *C. elegans* genome encodes for one syndecan, *sdn-1*, which is most similar the human syndecan-2. Syndecan has been shown to bind to DLar with high affinity during embryogenesis and synaptic development in *Drosophila* [7, 58]. LAR family members have also been shown to physically and genetically interact with HSPGs in Zebrafish trigeminal and Rohon-Beard neuron development [61]. In *C. elegans*, both *ptp-3* and *sdn-1* have been shown to function in multiple developmental events, including but not limited to, cell migration, synapse development and axon guidance [7, 15, 47, 62].

We found that in *C. elegans ptp-3* and *sdn-1* genetically function in parallel, and do not simply function in a one-to-one signaling pathway as in other organisms.

Although *ptp-3* and *sdn-1* single mutants each have a low level of embryonic or larval lethality *ptp-3;sdn-1* double mutants exhibit a highly penetrant synthetic lethality (SynLet). The majority of *ptp-3;sdn*-1 double mutants fail to enclose during embryogenesis or arrest during early larval stages. This combinatorial effect suggests that *ptp-3* and *sdn-1* function in parallel pathways essential for development.

Making use of the commercially available Ahringer RNAi library [63], we conducted an enhancer screen to identify secreted proteins using a SynLet approach. We screened ~3,600 predicted to encode for proteins present in the extracellular matrix or cell membrane using two strains containing a mutation in the *C. elegans* LAR homolog, *ptp-3* or the syndecan homolog, *sdn-1.* Using this reverse genetic approach allowed for the identification of genes that may have been missed in previous forward genetic screens due to partially penetrant phenotypes and/or redundant gene function.

Of the genes searched we isolated 25 genes that were SynLet with *ptp-3* alone, *sdn-1* alone, both *ptp-3* and *sdn-1*, and with our control strain alone. In particular, the Wnt ligand, *lin-44* displayed synthetic lethality with *sdn-1*. We also identified defects that have not been previously described in the organization and migration of endodermal precursor cells during gastrulation. These defects can be enhanced by the loss of *sdn-1*, suggesting that *lin-44* functions in a genetic pathway with *ptp-3* and in parallel to *sdn-1*.

Section 2.2 Introduction

Cell adhesion molecules (CAMs) provide multiple functions during the development and homeostasis of an organism. In *C. elegans,* multiple CAMs contribute to early embryonic development and loss-of-function (LOF) mutations in these can result in cellular, tissue and/or organismal abnormalities [64-67]. Interestingly, these molecules often appear to act in semi-redundant ways, where input from multiple CAMs are required for the fidelity of a specific developmental event [12, 14, 66, 68]. This can be best observed when LOF in a single gene has a modest effect on viability, but LOF in two genes in combination can have severe effects leading to highly penetrant lethality or arrest. This synergistic effect, known as Synthetic Lethality (SynLet), can be harnessed to uncover genetic interactions between functional pathways [69-75].

We and others have previously described developmental defects associated with *ptp-3,* the *C. elegans* Leukocyte-common antigen related (LAR)-like receptor protein tyrosine phosphatase (RPTP) [11-14, 76]. LAR is a member of the type IIa family of tyrosine phosphatases [10]. Vertebrates have three type IIa family members; LAR (PTPRF), RPTPσ (PTPRD) and RPTPδ (PTPRS) [77]. LAR-like RPTPs have been implicated in multiple aspects of nervous system development [78-85]. LAR is also required for proper mammary gland development in mice [86] and the LAR genomic locus is frequently deleted in breast, colon, and other cancers of epithelial origin [87]. Together, the pleiotropic nature of these observations highlights the

importance of LAR-like receptor tyrosine phosphatases in organismal development and homeostasis.

LAR-like RPTPs are receptors for extracellular matrix molecules, including laminin, chondroitin sulfate proteoglycans and heparan sulfate proteoglycans (CSPGs and HSPGs, respectively) [82, 88-90]. In *Drosophila* DLAR has been shown to bind syndecan and glypican, two cell-surface associated HSPGs [7, 58], consistent with reports from vertebrates demonstrating that LAR binds HSPG molecules [88, 90]. LAR family members have also been shown to physically and genetically interact with HSPGs in Zebrafish trigeminal and Rohon-Beard neuron development [61]. Importantly, *Drosophila* genetic studies, in addition to mammalian sensory neuron explant assays demonstrate that competition between distinct HSPG/CSPG ligands for LAR-like RPTPs can exert opposing effects on neural development [7, 90].

Syndecans are cell-surface associated HSPGs that have been implicated in a broad range of developmental events, and have been linked to the modulation of several secreted morphogens including Wnts and Fibroblast Growth Factors (FGFs) [91-98]. The extracellular domain of syndecans can be post-translationally modified with HS- or CS-side chains and the intracellular domain can interact with cytoplasmic signaling effectors via a PDZ binding motif. The *C. elegans* genome encodes a single syndecan, SDN-1, which, by sequence, is most similar to human syndecan-2 (SDC2) [15, 31, 99].

Here we provide genetic evidence that *ptp-3B* and *sdn-1* function in parallel signaling pathways during *C. elegans* embryonic development. *ptp-3; sdn-1* double

mutants exhibit a highly penetrant SynLet phenotype, with development arresting during embryogenesis or in the first larval stage (L1). A small percentage of animals do progress to adulthood, but exhibit sterility or low fecundity with all offspring arresting during development.

Using an RNAi library comprised primarily of predicted secreted proteins, we screened for genes that exhibited a SynLet phenotype with worms homozygous for either *ptp-3* or *sdn-1* LOF mutations. From a screen of 3,652 clones, we isolated 25 candidate SynLet genes, and several additional candidate genes displayed an increase in lethality or slow growth phenotype in either the *ptp-3* or *sdn-1* background, but did not meet our threshold criteria for synthetic lethality. Among the candidate genes, we found that the Wnt ligand, *lin-44,* was strongly SynLet with *sdn-1*, but not *ptp-3.* Using a time-lapse microscopy approach we found defects in the ingression of the endodermal precursor cells Ea and Ep in *lin-44* mutants. This phenotype was significantly enhanced when *sdn-1* was also removed. This is the first data indicating that LIN-44 contributes to gastrulation events in *C. elegans* and demonstrates the power of using double mutant analyses to uncover novel roles for well-characterized genes.

Section 2.3 Results

Dual loss of *ptp-3* and *sdn-1* results in synthetic lethality

Both *ptp-3* and *sdn-1* have previously described roles in *C. elegans* embryonic development [12, 14-16]. The *ptp-3* locus encodes three distinct transcripts, each with independent promoters [11] (Figure 2.1). Mutations in *ptp-3B* exhibit a low level of embryonic (Emb) and larval lethality (Lva) as well as Variable-abnormal body morphology defects (Vab) (Figure 2.2 and Table 2.1). However, most *ptp-3* LOF mutants are superficially normal in appearance. Similarly, *sdn-1* mutants exhibit low levels of Emb and Lva offspring (Table 2.1), but most grow to adulthood, where they exhibit uncoordinated movement (Unc) and egg-laying defects (Egl).

Based on the low penetrance viability defects in *ptp-3* mutants, and previous observations that the *Drosophila* LAR receptor, DLAR, can bind syndecan [7, 58], we asked whether *ptp-3* and *sdn-1* could be interacting genetically during *C. elegans* development. If PTP-3 and SDN-1 were acting as a ligand-receptor pair, we would have expected that *ptp-3; sdn-1* double mutants would exhibit embryonic lethality at a rate similar to the single mutant genetic backgrounds. In contrast we found that animals lacking both *sdn-1* and *ptp-3* were essentially inviable (Table 2.1). To score the development of these animals we generated *sdn-1(zh20)* homozygotes where a strong *ptp-3* LOF mutation, *mu245,* was balanced with a chromosomal inversion, *mIn1,* which is marked with a recessive mutation (*dpy-10),* and a dominant pharyngeal GFP insertion, *mIs14* (phGfp) (see Materials and methods).

We found an increase in the embryonic and larval lethality in offspring from *sdn-1(zh20); ptp-3(mu245)juIs76/mIn1mIs14* mothers compared to *sdn-1(zh20);*

juIs76 or *ptp-3(mu245)juIs76* alone. Compared to the expected 25% of the brood, only 12.6% of live hatchlings were *ptp-3; sdn-1* (126/1000 offspring from a total of 5 mothers). Further, when these broods were analyzed on the first day of adulthood, only 2% (2/114 offspring) of the adults were *sdn-1(zh20); ptp-3(mu245)juIs76*). Surviving *sdn-1(zh20); ptp-3(mu245)juIs76* adults appeared sickly, were largely paralyzed and had no viable offspring (78 Emb and 5 Lva L1s from 4 mothers). SynLet phenotypes were also observed when we tested other strong *ptp-3* LOF mutations including *ptp-3(mu256)* and *ptp-3(op147)*, and a second deletion allele in *sdn-1, ok449.* None of the *ptp-3; sdn-1* double mutant combinations were viable as homozygous strains, and each had to be maintained as balanced *ptp-3/mIn1mIs14* heterozygotes for propagation. In addition, RNAi targeting *sdn-1* was lethal in *ptp-3(mu245)* animals, and RNAi targeting *ptp-3* was lethal in *sdn-1(zh20)* animals. These data confirm that the SynLet phenotypes observed are due to the alleles in question and not caused by closely linked background mutations.

We more closely analyzed the *sdn-1(zh20); ptp-3(mu245)* homozygous animals to determine the point at which they were arresting. We found instances of early embryonic arrest (pre-morphogenesis), embryonic rupture during epidermal enclosure, and arrest at the L1 stage as misshapen larvae. These are similar arrest points to those observed in embryos from *sdn-1(zh20); ptp-3(mu245)/mIn1mIs14* mothers. However, the higher rate of embryonic arrest in the offspring of *sdn-1(zh20); ptp-3(mu245)* animals than from *sdn-1(zh20); ptp-3(mu245)/mIn1mIs14* mothers strongly suggests a maternal contribution of *ptp-3* to embryonic development. Since the offspring of *sdn-1*(*zh20); ptp-3(mu245)* animals, which

should lack any maternal contribution, demonstrated a variable arrest point, we concluded there are likely several stages of development to which both SDN-1 and PTP-3 contribute, in partially compensatory ways. However, we cannot completely discount that defects that occur early in development may present as variable arrest phenotypes. Overall these results indicate that *ptp-3* and *sdn-1* have overlapping function during embryogenesis and that loss of both genes results in dire consequences for organismal survival.

We previously demonstrated that two of the isoforms produced by the *ptp-3* locus have differential localization [11, 12]. PTP-3A localization is restricted to synapses, while PTP-3B is associated with cell-cell junctions during embryogenesis but also localizes to axons during axon outgrowth. Consistent with their different localizations, PTP-3A and PTP-3B appear to function as distinct genetic units as loss of *ptp-3A* has no embryonic patterning or axon guidance defects, yet exhibits a fully penetrant synaptic morphology defect that is equivalent to a complete loss of function for the *ptp-3* locus [11]. Similarly, PTP-3B is capable of rescuing the embryonic development, cell migration and axon outgrowth defects associated with *ptp-3* LOF mutations [9, 12, 13, 64]. The *ptp-3(mu245)* lesion specifically affects the PTP-3A and PTP-3B isoforms, and we did not observe a SynLet phenotype when we used a LOF mutation in *ptp-3* that specifically affects the PTP-3A isoform, *ptp-3A(ok244)* (Figure 2.1). This is consistent with our previous results suggesting that PTP-3A does not obviously contribute to epidermal development, while PTP-3B does.

To better understand what might be contributing to *ptp-3; sdn-1* lethality during embryogenesis, we used 4D time-lapse microscopy to observe cell division and migration during the first 10 hours of embryonic development. The first cell migration event that occurs during *C. elegans* development is the onset of gastrulation, where the gut precursor cells, Ea and Ep, ingress into the center of the embryo [29]. In wild-type embryos, Ea and Ep ingress in concert, side-by-side, with the space vacated by their ingression filled by movements from six surrounding cells [100]. The next major developmental event occurs when cells of the endodermal and mesodermal lineage begin to ingress at the posterior end, leaving a transient gastrulation cleft on the ventral surface (Figure 2.3) [101]. Onset of cleft opening was phenotypically normal in the embryos observed (n = 10) although one embryo showed a gastrulation cleft opening at the anterior end. However, the relative timing of gastrulation cleft opening was significantly delayed in *ptp-3* embryos when compared to Ea/Ep ingression and comma stage. The gastrulation cleft is flanked by neuroblasts; in wild-type embryos, these normally migrate towards the midline of the ventral surface, closing the cleft in about 55 minutes [16]. These subsequently form a substrate for epithelial cell migration, which intercalate and extend from the dorsal and lateral surfaces to enclose the embryo during epiboly.

In *ptp-3; sdn-1* mutants, 8/14 embryos showed gastrulation clefts that persisted until epithelial extension and ventral enclosure (Figure 2.3). All of these embryos ruptured prior to comma stage, at the onset of embryonic elongation (class I phenotype, [102]). Two large cells were frequently seen in the center of these

enlarged clefts that showed no adhesion to the cells surrounding them. Based on previous cell lineage experiments, we tentatively identified these as the germ line precursor cells Z2 and Z3 (M. L. Hudson, unpublished observations). Additional embryos showed gross disorganization during development, with lateral loss of cell – cell contacts on the embryo surface prior to cleft opening. In the embryos that survived ventral enclosure, defects were also observed in tail morphology. While gastrulation cleft opening appears to be significantly delayed in *ptp-3; sdn-1* mutants compared to *ptp-3* alone, only 3/10 *ptp-3; sdn-1* mutants could be scored for this phenotype as most embryos rupture prior to reaching comma stage, and hence cannot be scored for the final developmental timeline marker. As such, this apparent suppression of *ptp-3* developmental timing defects may be misleading. Overall, the most common cause of embryonic lethality was failure to close the gastrulation cleft prior to ventral enclosure. These data confirm previously identified roles for SDN-1 and PTP-3 in embryonic morphogenesis [12, 16], and suggest that SDN-1 and PTP-3 function in parallel, part-redundant pathways to control either cell adhesion, neuroblast migration or both.

An RNAi screen for SynLet interactions with *ptp-3* and *sdn-1*

The observation that simultaneous LOF in *ptp-3* and *sdn-1* resulted in a highly penetrant SynLet phenotype suggested that we could use these backgrounds to identify additional genes that contribute to embryonic development [69]. We employed RNAi knockdown to systematically screen for genes that lead to a synergistic SynLet phenotype in either *ptp-3(mu256)* and/or *sdn-1(zh20)* mutant

backgrounds. RNAi clones that were identified from the first round of screening were retested at least four times to confirm the results. The threshold for declaring an interaction as synthetic lethal was >75% Emb. We also identified genes that were SynLet with both *ptp-3* and *sdn-1,* suggesting these may function in yet another independent parallel pathway, or may contribute in overlapping fashion to both the *ptp-3* and *sdn-1* pathways.

We found 11 genes that showed a SynLet phenotype in *ptp-3(mu256)* animals, but only limited or no lethality in a wild type background (Table 2.2, Supplemental Table 1). Two of these genes, *vab-1* and *unc-40,* have previously been found to be SynLet with *ptp-3,* indicating that our screen was capable of identifying relevant genetic interactions [12-14, 31]. We also found genes that are known to be individually lethal via complete loss-of-function mutations, including *bli-3* and *mek-2.* However, in our assays, RNAi knockdown in the wild type background was insufficient to cause highly penetrant lethality. We conclude that this approach enabled us to identify genetic interactions that might be missed using traditional loss-of-function alleles.

Seven of the genes found to be SynLet in the *ptp-3* background had an attenuated effect when knocked down in the *sdn-1* background (Table 2.2). These genes are candidates to function in *sdn-1* mediated development. Of these, several have been associated with the formation or function of the nervous system (including *unc-40, vab-1, mek-2* and C27C7.5). Because syndecans are associated with neural development it suggests either failures in neural development can interfere with normal embryogenesis, or that these molecules perform non-neural

developmental functions, with more evidence for the latter [65, 103]. A second theme that emerged when analyzing the list of candidate genes is that several of the genes have an association with gametogenesis or the germline. For example, *perm-4* is expressed in oocytes, and regulates an interaction with sperm, while the C04F12.7 gene is co-expressed with several sperm-specific genes. VAB-1 has also been linked to the function of germline maintenance [104]. Finally, the ZC190.5 has been previously identified as a suppressor of the *egl-9* locus [105]. EGL-9 encodes a proline hydroxylase that negatively regulates HIF-1 signaling [106], but also participates in neural development [107]. Thus, it will be interesting to determine whether the identification of these genes implicates syndecan in oxygen sensing or germline development/function.

We isolated 15 clones that generated a SynLet phenotype in *sdn-1* mutants, but had no effect, or an attenuated one, when knocked down in *ptp-3* animals. One of the most interesting candidates to emerge was the Wnt ligand, *lin-44* (see below). Wnt ligands contribute to multiple facets of organismal development throughout the animal kingdom. Interestingly, a recent paper describes an interaction between *sdn-1* and another *C. elegans* Wnt ligand, *mom-2,* where SDN-1 concentrates the MIG-5/Dishevelled protein in early embryogenesis [30].

We also identified several genes that may contribute to post-translational modifications of proteins, possibly including Wnts, such as an O-acyltransferase (*oac-9)*, a mannosidase (*mans-1),* a pterin-4-β-carbinolamine dehydratase (*pcbd-1*), a putative sugar transporter (B0041.5), a subtilisin-like endoprotease (*bli-4*) and a dual-oxidase (*bli-3*). It should be possible to use the *lin-44 – sdn-1* interaction we

describe below to tease out potential contributions of these molecules to Wnt-dependent functions. Two of the genes are likely involved in mitochondrial function (*stl-1,* and F43G9.3), although it is unclear whether this function is contributing to the embryonic lethality when knocked down in *sdn-1.*

An unanticipated outcome of the RNAi SynLet screen was the discovery of three genes where RNAi was lethal to our control strain yet showed incomplete penetrance in *ptp-3* or *sdn-1* mutant backgrounds. Two of those genes, C18B12.4 and *mnp-1* are reported to cause lethality when mutated, or when knocked down in wild-type animals via RNAi [108-111]. The third gene, F17B5.6, is predicted to code for a glycosyl transferase and has not previously been reported to have a role in embryonic development. *mnp-1*, which encodes a 781 amino acid protein related to the M1 family of metalloproteinases, is required during embryonic development to facilitate muscle cell migrations from lateral to dorsal and ventral positions [111]. Previous work has demonstrated that *mnp-1* genetically interacts with the Eph Receptor *vab-1,* which is SynLet with *ptp-3,* suggesting that the interactions between these genes maybe more complicated than previously suggested. Interestingly, *mnp-1* is predicted to be catalytically inactive due to the lack of three of four essential zinc-binding amino acids, and thus may function in more of a structural role, perhaps by occluding peptidase sites to promote structural integrity.

In the course of our screen we found other genes that interacted genetically with *ptp-3* and/or *sdn-1,* but these interactions were either too variable, or did not repeat in multiple assays, to formally conclude their role in embryonic and larval development (Supplemental Table 1). Some of these caused slowed growth (Gro) or

an apparent sickness (Sck) that lead to decreased viability over the experimental window, while others may have caused increased changes in the body morphology defects (Bmd or Vab) (Supplemental Table 1). Although these were not included in the list of SynLet candidates, the genes may merit analysis in the future when attempting to further understand how PTP-3 or SDN-1 contribute to morphogenesis.

Epidermal junction defects do not correlate with SynLet phenotypes

PTP-3B is associated with cell junctions during the cellular migrations and tissue rearrangements that occur during embryogenesis, and *ptp-3B* mutants exhibit low-penetrance epidermal morphology (Vab) defects [12]. SDN-1 also localizes to the plasma membrane, being concentrated at cell-cell junctions in early embryos [30]. We hypothesized that lethality might arise from disruption of epidermal junction formation or patterning. To assay this we examined a marker for epidermal junctions, AJM-1::GFP, in *sdn-1* or *ptp-3* mutants alone and when grown on enhancer gene RNAi expressing bacteria.

In wild type animals, AJM-1::GFP can be seen accumulating at cell junctions outlining the epidermal cells, starting around the lima bean stage of embryogenesis, and persisting throughout development (Figure 2.4). Epidermal cell junctions in wild-type animals are well organized, and only rarely display gaps or misshapen cells. In contrast, we found that both *ptp-3* and *sdn-1* mutants had apparent cell-shape changes consistent with defects in either cell positioning or cell polarity (Figure 2.4, Table 2.3).

Interestingly, the presence of disorganized cells as visualized by AJM-1::GFP did not correlate with the embryonic or larval lethality in the various mutant backgrounds assayed. For example, only 4% (4/100) *ptp-3* mutants had obvious defects in the AJM-1::GFP pattern (Table 2.3). In contrast, 87% (87/100) of *sdn-1* mutants exhibited abnormalities in AJM-1::GFP expression. Despite this, the rate of embryonic lethality in these two backgrounds is similar. Also, when we used RNAi to knock down gene expression in our SynLet screen, we found no correlation between the effect of RNAi on embryonic development and changes in the expression pattern of the epidermal junction marker. Overall this suggests that while these genes may contribute to the positioning of epidermal cells or the organization of epidermal junctions, the proper localization of AJM-1::GFP to these sites is insufficient to explain the lethality observed in the different genetic backgrounds. This is similar to previous reports for cell adhesion molecules in *C. elegans*, *e.g.* loss of the E-cadherin-like HMR-1, results in lethality, but animals can form and maintain intact epidermal junctions [112].

The Wnt ligand LIN-44 functions in gastrulation

One of the strongest SynLet interactions uncovered in our screen was between the Wnt ligand *lin-44* and *sdn-1* (Figure 2.3, Table 2.1). Wnts and syndecan have been shown to function together in multiple developmental contexts in both *C. elegans* and other systems [31, 98, 113, 114]. The *C. elegans* genome encodes five Wnt ligands; *cwn-1, cwn-2, egl-20, lin-44* and *mom-2.* Of these only *mom-2* has been shown to function in embryonic development, as loss of function in *mom-2* results in

maternal-effect embryonic lethality [100], although loss of multiple Wnts can result in a more penetrant lethality [115]. In our screen, knockdown of *lin-44* caused a robust increase in the embryonic and larval lethality of *sdn-1* mutants, but not in *ptp-3* or wild-type animals. We did not observe lethality in *sdn-1* animals treated with *egl-20* or *cwn-2* RNAi, while *mom-2* knockdown caused embryonic lethality in all backgrounds tested. *cwn-1* was not present in our RNAi library hence was not assayed.

To better understand the morphogenetic defects behind the *lin-44* and *sdn-1* interaction, we built and analyzed a double LOF line, *lin-44(n1792); sdn-1(zh20)*. *lin-44(n1792)* is predicted to be a complete loss of function mutation at the *lin-44* locus, hence this strain was genetically null for both genes in question. We found that *sdn-1; lin-44* double mutants showed a significant increase in the penetrance of embryonic lethality compared to either single mutant (Table 2.1).

Using time-lapse video microscopy, we found highly penetrant defects in the migration of endodermal precursor cells Ea and Ep, in *lin-44; sdn-1* double mutants at the 24-cell stage of development (Figure 2.5). In wild type animals gastrulation begins when Ea and Ep rotate and then ingress from the surface of the embryo to the center [51]. In *lin-44; sdn-1* double mutants, 48% of embryos (11/24) showed defective Ea/Ep ingression, compared to 21% of *lin-44* (5/23) and 20% of *sdn-1* (3/15) single mutant embryos. As a comparison, we also examined *ptp-3; sdn-1* embryos for Ea/Ep ingression failure. 29% (2/7) embryos showed defects in this process. In one embryo, the Ea/Ep cells completely failed to ingress, while in another, Ep ingressed before Ea. These data are not significantly different from *sdn-*

1 mutants alone, suggesting that *ptp-3* has no obvious role in early gastrulation. These defects in Ea/Ep ingression often resulted in endodermal cells appearing on the embryo's surface later in development (Gut on the exterior, or Gex phenotype), with catastrophic consequences for subsequent epithelial cell migrations (Figure 2.5). Further analysis of our time-lapse data revealed that 15% (3/20) of *lin-44* embryos showed defects in neuroblast migration as manifested by an increase in gastrulation cleft duration and failure of epithelial cells to enclose the embryo (Figure 2.5). This is likely due to mis-positioned gut cells inhibiting or blocking epithelial cell migrations, or causing defects in overall embryonic organization. While the *lin-44; sdn-1* Ea/Ep ingression phenotypes appear to be additive when compared to each single mutant, the increase in embryonic lethality is clearly synergistic (Table 2.1). As such, it appears that small defects in Ea/Ep ingression early in development lead to severe consequences in later developmental events. Together these results indicate that both *lin-44* and *sdn-1* contribute to the normal migration of Ea and Ep cells at the onset of gastrulation, and that *ptp-3* has no obvious role in this process. In addition, both *lin-44* and *sdn-1* may also be involved in controlling neuroblast migration and gastrulation cleft closure later in embryogenesis, although in the case of *lin-44*, we cannot rule out that defects at later time points are a consequence of earlier defects in Ea/Ep migration.

In other contexts LIN-44 has been shown to signal through the LIN-17 Frizzled-like receptor. We made double mutants of *lin-17* with *sdn-1,* but found no significant increase in the Emb phenotype compared to *sdn-1* animals alone (Table 2.1). *lin-17; sdn-1* double mutant adults were strongly Unc, and often died early,

around day 2-3 of adulthood, compared to *sdn-1* adults, which live for ~7-10 days (B.D. Ackley unpublished observations). This suggests that LIN-44 affects gastrulation via a different receptor, and does not specifically function via LIN-17.

Finally, we examined whether *ptp-3* loss of function also synergized with *lin-44.* We found that double mutants of *ptp-3(mu245); lin-44(n1792)* exhibited Emb lethality at a rate similar to *ptp-3(mu245)* single mutants (Table 2.1), although there was a slight increase in larval lethality in the double mutants compared to each single mutant background. This suggests that *lin-44* and *ptp-3* may be functioning in the same genetic pathway during embryonic development. Overall, our results are consistent with *ptp-3* contributing to *lin-44*-dependent gastrulation, and that at least one of the potential reasons that *ptp-3; sdn-1* double mutants die is because of a disruption in the *lin-44 / ptp-3* signaling pathway.

Section 2.4 Discussion

Embryonic development requires an orchestrated set of cell migrations and rearrangements, and the proper modulation of cell adhesion is critical to this process. Here we have demonstrated that the type IIa RPTP, *ptp-3* and the syndecan ortholog, *sdn-1,* contribute to parallel genetic pathways during *C. elegans* embryogenesis. The dual loss of these molecules results in developmental failure due to defects in two major cellular rearrangements, gastrulation and epiboly. Both *sdn-1* and *ptp-3* have roles at the onset of gastrulation, which is the first major cellular rearrangement seen in *C. elegans* development. In addition, both are clearly required for cell migration events later in development at gastrulation cleft closure. Failure to close the gastrulation cleft leads to subsequent defects in hypodermal enclosure and developmental failure via ventral rupture at the onset of embryonic elongation.

At first glance our results seem at odds with data from other organisms, where LAR-RPTPs and syndecans have been found to function as a ligand-receptor pair [7, 58]. In the *Drosophila* neuromuscular junction, cis-interactions on the neural membrane between DLar and syndecan interfere with trans-interactions between neural DLar and muscle-derived glypican. The binding of DLar to syndecan reduces the adhesion at the NMJ and serves to permit expansion of the structure. However, the *C. elegans* isoform most similar to DLar, shown to bind syndecan, is PTP-3A, which is genetically and functionally distinct from the isoform we found to cause embryonic defects, PTP-3B. In our assays *ptp-3A* had no effect on embryonic

viability, either alone or in combination with *sdn-1,* suggesting that the differences between our observations and others are due to the isoform being analyzed.

The PTP-3B isoform that our data implicate as functioning in parallel to SDN-1 appears to be conserved evolutionarily in vertebrates, but is not obviously found in *Drosophila.* In vertebrates a short isoform of the LAR/PTP-3F receptor has been identified that has the same domain architecture as PTP-3B, being comprised of 5 Fibronectin type III domains in the extracellular portion and two tandem phosphatase domains intracellularly (Uniprot - H0Y4H1). Thus, it is possible that the interaction we have observed between LAR and syndecan is conserved in vertebrates as well.

Our results suggest that in *C. elegans* embryonic development, the syndecan and LAR proteins have overlapping roles, and can partially compensate for the absence of each other. Further, we found that animals lacking both *ptp-3* and *sdn-1* exhibited variable points of developmental arrest. This was most apparent in the animals that lacked any maternal *ptp-3* contribution, which arrested embryogenesis during epiboly or at hatching, after completing embryogenesis. The variable arrest points of the *sdn-1; ptp-3* double mutants suggests that there are likely multiple phases of development in which SDN-1 and PTP-3 function in parallel to provide essential functions. However, an alternative hypothesis is that an early defect at the onset of gastrulation can lead to a variable arrest point later in development. Based on our time-lapse analysis, our data favor the former, but it is possible that subtle defects during early development are occurring. To address this point we will need

to identify the mechanism(s) that underlie the lethality of the *ptp-3; sdn-1* double mutant animals.

Additional factors likely provide some compensatory function in the absence of both PTP-3 and SDN-1, permitting animals to get through critical developmental periods. For example, some *sdn-1; ptp-3* embryos fail to complete epiboly; if this were the earliest function of PTP-3 and SDN-1, and they could not be compensated for during this process, we would expect 100% of the embryos to arrest at that point in development. However, we find that some animals complete epiboly, but arrest at a later time point. The variable arrest points seen in the double mutants suggest that there are potentially multiple proteins that could partially compensate for the loss of *ptp-3* and/or *sdn-1* during development, including the Eph-ephrin, and slit-robo pathways, which have previously described roles in this process [14, 68, 102].

The SynLet phenotype observed in *ptp-3; sdn-1* double mutants provided us with a powerful platform to identify novel genetic interactions required for embryonic development. We found that we can induce lethality in either the *ptp-3* or *sdn-1* mutant backgrounds by knockdown of orthogonal genes using RNA interference (RNAi). Like most screens using RNAi we observed some variability in the efficacy, compared to known loss-of-function mutations. While this may complicate the interpretation of epistatic relationships, we found RNAi had a robust effect for the purposes of discovery.

Based on the results of our SynLet screen, we propose that there are at least three, and likely more, different cell-adhesion pathways functioning semi-redundantly during *C. elegans* development, at least two of which utilize *ptp-3* and

sdn-1. This is not surprising, as development requires an integrated symphony of cell movements, wherein adhesion must be transiently changed in an orchestrated fashion. However, it is interesting to note that some cell adhesion proteins, *e.g.* laminin, perlecan, collagen IV and integrins are categorically essential to embryonic viability, whereas others, like *ptp-3* or *sdn-1*, have a more flexible requirement. As laminin, perlecan and collagen IV are all components of the basal lamina, and integrins receptors for some of these proteins, it suggests that the basal lamina is a crucial reference point for cell migrations. Cell adhesion, via proteins like PTP-3B or SDN-1, appears to be a more redundant process, with multiple proteins capable of contributing to this role.

Our SynLet screen has identified multiple genes with previously undiscovered roles in embryonic development. The identification of *mnp-1* as a suppressor of *ptp-3* and *sdn-1* lethality suggests a complex interplay between cell adhesion and matrix remodeling proteins during embryogenesis. The Eph receptor *vab-1* has previously been shown to function in parallel with *mnp-1* during *C. elegans* embryonic muscle cell migration [111]. *vab-1* also functions in parallel with *ptp-3* to regulate epidermal migration during morphogenesis [12]. The genetic interactions we observe suggest that loss of *ptp-3* was protective to animals where *mnp-1* had been knocked down. Thus, it will be interesting to determine if this reveals a previously unknown role for *ptp-3* in muscle cell migration, or a role for *mnp-1* in epidermal cell migration.

One of the interactions we uncovered using our SynLet RNAi approach was a genetic interaction between *sdn-1* and *lin-44*, one of the five Wnt ligands encoded by

the *C. elegans* genome [44]. Prior to this, *mom-2* was the only Wnt ligand that had been demonstrated to affect gastrulation. However, it has been shown that in other Wnt ligands can influence this as *cwn-1* and *cwn-2* mutations enhance the *mom-2* lethal phenotype. The fact that the *cwn-1;cwn-2;mom-2* triple mutants exhibit a fully penetrant lethality indicates at least some functional redundancy of Wnt ligands in embryogenesis [115]. *mom-2* contributes both to endodermal specification and gastrulation through partially overlapping functions [100]. Ultimately, MOM-2, functioning through the frizzled-like receptor MOM-5, results in the phosphorylation of myosin light chain to induce constriction of the apical surfaces of the Ea and Ep cells to induce their internalization. Recent work has also uncovered a novel role for SDN-1 in embryogenesis, where it functions in a MOM-2-dependent pathway to control the orientation of the mitotic spindle earlier in embryogenesis (6 to 8 cell stage of development) [30].

Here we find that *lin-44* also affects the internalization of the Ea and Ep cells, albeit to a lesser extent than *mom-2.* The loss of *sdn-1* significantly enhances the penetrance of Ea and Ep ingression defects, and synergistically causes a highly penetrant embryonic lethality. Further, genetic evidence suggests that the LIN-17 frizzled-like receptor does not function in this event, although previous reports have generally found that LIN-44 signals through LIN-17 [116-120].

Previous work suggested that LIN-44 appears to prime cells for other Wnt-signals. For example, in the PLM mechanosensory neurons, LIN-44 activity was required to induce asymmetric localization of LIN-17 which then acted as a receptor for the EGL-20 Wnt ligand [117, 120]. One possibility is that LIN-44 also primes the

Ea and Ep cells to respond to the MOM-2 ligand, although this remains to be determined.

The use of parallel genetic backgrounds to identify SynLet interactions allowed us to immediately assign a candidate gene into a genetic pathway, based on the outcome of the screen. For instance, *lin-44* RNAi knockdown strongly enhanced *sdn-1* LOF phenotypes, yet showed no synergistic phenotypes in a *ptp-3* mutant background. This suggests that *ptp-3* somehow functions in the Wnt pathway during *C. elegans* embryonic development. Interestingly though the *lin-44; ptp-3* double mutants did have an increase in larval lethality over the single mutant backgrounds, although it did not result in complete synthetic lethality as nearly 70% of the animals survived to adulthood. This may indicate though that during larval development *ptp-3* and *lin-44* function in parallel pathways. Our future studies harness *sdn-1* synergistic effects to allow us to further explore the mechanisms by which *lin-44* and *ptp-3* affect gastrulation in *C. elegans.*

Section 2.5 Materials and Methods

Genetics

The following alleles were used in this report: N2 (var. Bristol), *sdn-1(zh20), sdn-1(ok449), ptp-3(mu254), ptp-3(mu256), ptp-3A(ok244), ptp-3(op147), lin-17(n671), lin-44(n1792), eri-1(mg366), juIs76* [*Punc-25::gfp*], *jcIs1* [P*ajm-1*::AJM-1::GFP] and *mIn1mIs14.* Strains were maintained at 18-22 ºC, using standard maintenance techniques as described [121]. All lethality counts were conducted with animals maintained at 20 ^{0}C.

To score the synthetic lethality of the *ptp-3; sdn-1* double mutant animals we generated *sdn-1(zh20)* homozygotes where *ptp-3*(*mu245),* was balanced with a chromosomal inversion, *mIn1,* which is marked with a recessive mutation (*dpy-10),* and a dominant pharyngeal GFP insertion, *mIs14* (phGfp). We further marked the *mu245* lesion by linking it to a GABAergic neuronal marker, *juIs76* [*Punc-25::gfp*] (nGfp). Progeny from the *sdn-1(zh20); ptp-3(mu245)juIs76/mIn1mIs14* mothers were expected to define the following three phenotypic classes and their corresponding genotypes:

Dpy+phGfp - (*sdn-1(zh20); mIn1mIs14/mIn1mIs14*)

phGfp+nGfp+NonDpy - *(sdn-1(zh20); ptp-3(mu245)juIs76/mIn1mIs14)*

NonDpy+NonphGfp+nGfp - *sdn-1(zh20); ptp-3(mu245)juIs76.*

RNAi feeding control strains used

RNAi clones were compiled from the Ahringer library [63]. Three RNAi controls were used during each round of screening, an empty vector (L4440), and

clones targeting *ptp-3* (II-7J03; Overlapping CDS: C09D8.1) or *sdn-1* (pEVL202). The *sdn-1* fragment designated for RNAi was obtained by polymerase chain reaction (PCR) from N2 genomic DNA. The fragment was then cloned into the pCR8 TOPO cloning vector (Life Technologies) and recombined via an LR reaction into a L4440 feeding vector. The resulting plasmid was transformed into the HT115(DE3) RNase III-deficient *E. coli* strain. The following primer pairs were used for PCR amplification of *sdn-1*: forward 5'-TTTTCTTTTAGAACCCTTTTGC-3' reverse: 3'-CATCAATTTATCATCTCGCAAC-5'.

RNAi feeding assay (6-well format)

HT115 bacterial strains, containing the RNAi clones of interest, were grown overnight at 37 °C in 1.5 mL LB plus ampicillin, tetracycline and nystatin. 100 µl of the overnight cultures were aliquoted on single 6-well plates of NGM containing carbenicillin, tetracycline, and 1mM IPTG and grown overnight at 37 °C. Approximately 3-4 L4 worms were dispensed in M9 into the top wells (1, 2 and 3) on the 6-well plates. The plates were left at approximately 20 °C for five days before the worms were scored for phenotypes and 3-4 L4 worms were transferred to the bottom wells (4, 5 and 6). The bottom wells were then scored after six more days. The experimenter was blind to the RNAi clone being tested in all assays. All clones that exhibited any level of SynLet were rescreened as described above to verify the interaction. Clones were then rescreened if they displayed SynLet or slow growth with any of the query strains. We categorized SynLet as embryonic lethal (Emb), larval lethal (Lvl) or adult lethal (Adl). The following additional phenotypes were

also scored: Lethal (Let), body morphology defects (Bmd), uncoordinated (Unc), sickness (Sck), sterility (Ste), slow growing (Gro), protruding vulva (Pvl), dumpy (Dpy) and/or egg laying defective (Egl). All phenotypes were compared between the strains on that 6-well plate alone.

RNAi clone sequencing

Clones isolated from the screen were grown as single clones in liquid LB cultures containing ampicillin, tetracycline and nystatin. Cultures were purified using a Qiagen spin mini-prep kit then sequenced using a modified forward T7 primer (5'-ACTCACTATAGGGAGACCGG-3').

Time-lapse microscopy of embryonic development

4-dimensional video microscopy was carried out using an Olympus BX61 microscope equipped with a 63x magnification oil immersion objective and motorized z-axis stage. Z-stacks (27-35 slices) were collected every 2 minutes at 1 micron spacing using a Retiga camera (Q-Imaging). Data sets were analyzed via the Bioformats-Importer and 4D Browser plugins in ImageJ [122, 123]. The following time points were collected; Ea/Ep ingression, gastrulation cleft opening, cleft closure, and comma stage. Analysis of developmental time points was normalized relative to Ea/Ep ingression and comma stage. Embryonic lethal phenotypes were categorized according to [102]. Ea/Ep ingression behavior was scored as follows; I, normal (Ea/Ep ingress together); II, no ingression (Ea/Ep remain on the outer surface of the embryo); III, skewed (either Ea or Ep ingresses before its partner); IV,

unclassified (Ea/Ep migration obscured or unclear). (4d analysis was conducted by Dr. Martin Hudson at Kennesaw State University.)

Lethality analysis

A single L4 hermaphrodite was placed on a single NGM plate to initiate the assay. Every 24 hours the hermaphrodite was transferred to a new plate. 24 hours after the removal of the hermaphrodite the plate was analyzed for embryos (Emb) or dead L1 larvae (Lva). The plate was rescreened 24 hours later for later larval lethality (Lva). Adults were transferred until they died, or until they stopped giving rise to offspring. All animals were maintained at 20 ^{0}C, except during scoring. Experimenter was blind to the genotype during scoring. (Lethality analysis was conducted by Dr. Brian Ackley.)

Epithelial morphology assays

Epithelial tight junctions were visualized with *jcIs1 [ajm-1::GFP],* which localizes to epithelial junctions, essentially outlining all epithelial cells from about the lima bean stage onwards. Multiple embryos were harvested by bleaching and > 100 assayed for epithelial morphology. Embryos that had cells that were obviously mis-positioned, *e.g.* dorsal cells on ventral side, or misshapen in a way that was strikingly different from wild-type, *e.g.* rounded cells along lateral aspect where cuboidal cells are normally present, were scored as a mutant. We also recorded time-lapse movies of embryonic development using a Zeiss LSM700 confocal microscope. (Time-lapse

data was recorded by Dr. Martin Hudson and epithelial analysis conducted by Curtis Yingling.)

Section 2.6 Figures

Figure 2.1

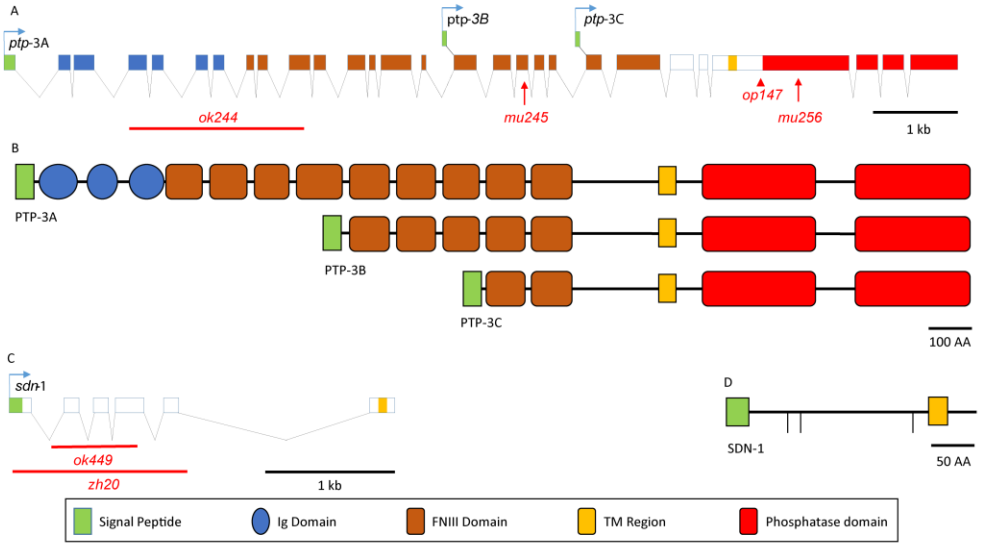

Figure 2.1 Genomic and protein structure of *ptp-3* and *sdn-1* A schematic of the gene and protein structures of *ptp-3* and *sdn-1* are presented with lesions used in this report indicated. (A) The *ptp-3* genomic locus gives rise to at least three independently generated transcripts, *ptp-3A, ptp-3B* and *ptp-3C.* The *ptp-3(ok244)* deletion specifically affects *ptp-3A*, *ptp-3(mu245)* is a premature stop that affects *ptp-3A* and *ptp-3B, ptp-3(op147)* is a Tc1 transposon insertion and *ptp-3(mu256)* is a frameshift and premature stop that affects all three transcripts. (B) The three PTP-3 protein isoforms differ by the composition of the extracellular domains. See key at bottom of figure for domain architecture. (C) The *sdn-1* genomic locus produces a single transcript. The two deletion alleles, *sdn-1(zh20)* and *sdn-1(ok449),* both remove a large portion of the *sdn-1* coding segment and are strong loss of function alleles. (D) The SDN-1 protein has three SG motifs (vertical lines) that are predicted to be targets for the addition of heparan sulfate side chains.

Figure 2.2

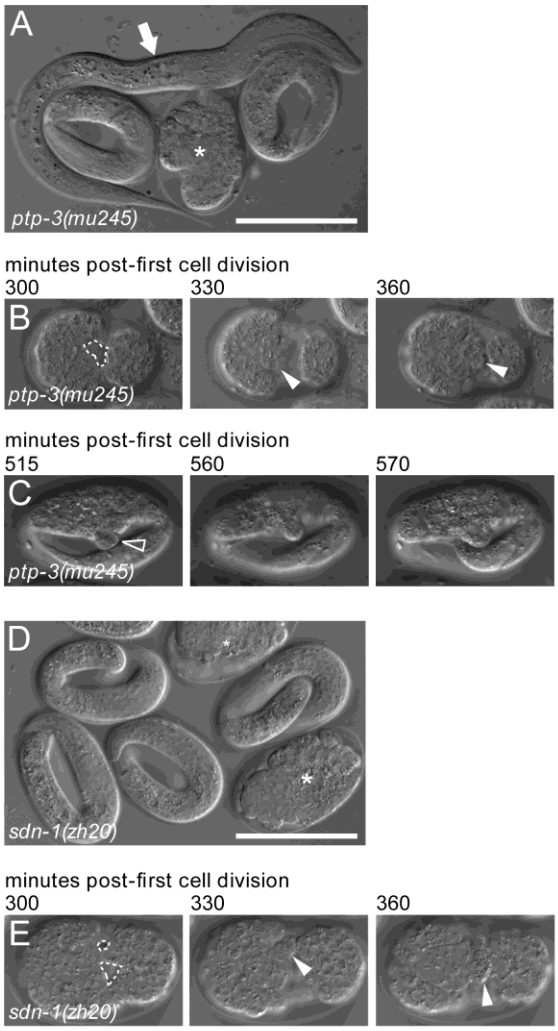
A
ptp-3(mu245)
minutes post-first cell division
300
330
360
B
ptp-3(mu245)
minutes post-first cell division
515
560
570
C
ptp-3(mu245)
D
sdn-1(zh20)
minutes post-first cell division
300
330
360
E
sdn-1(zh20)

Figure 2.2 Loss of function in *ptp-3* and *sdn-1* results in low penetrance embryonic and larval defects (A) *ptp-3(mu245)* mutant animals can hatch as normal looking L1 larvae (arrow), but can also die during embryogenesis (asterisk shows an embryo that ruptured at elongation). (B) *ptp-3* mutants can exhibit defects in ventral neuroblast migration (B1 outlined area), which result in a persistent gastrulation cleft on the ventral surface. When these fail to close, internal cells extrude through the opening (arrowheads) during elongation, leading to embryonic lethality. (C) *ptp-3* mutants can also exhibit variably abnormal herniations in body morphology (empty arrowhead). (D) *sdn-1(zh20)* mutants also exhibit low penetrance embryonic lethality (asterisks show ruptured embryos). (E) Gastrulation cleft closure defects are observed in some *sdn-1(zh20)* mutant embryos (outlined area). Again, this can lead to embryonic rupture at ventral enclosure (arrowhead shows cells oozing from within). (Image acquisition and analysis done by Dr. Martin Hudson.)

Figure 2.3

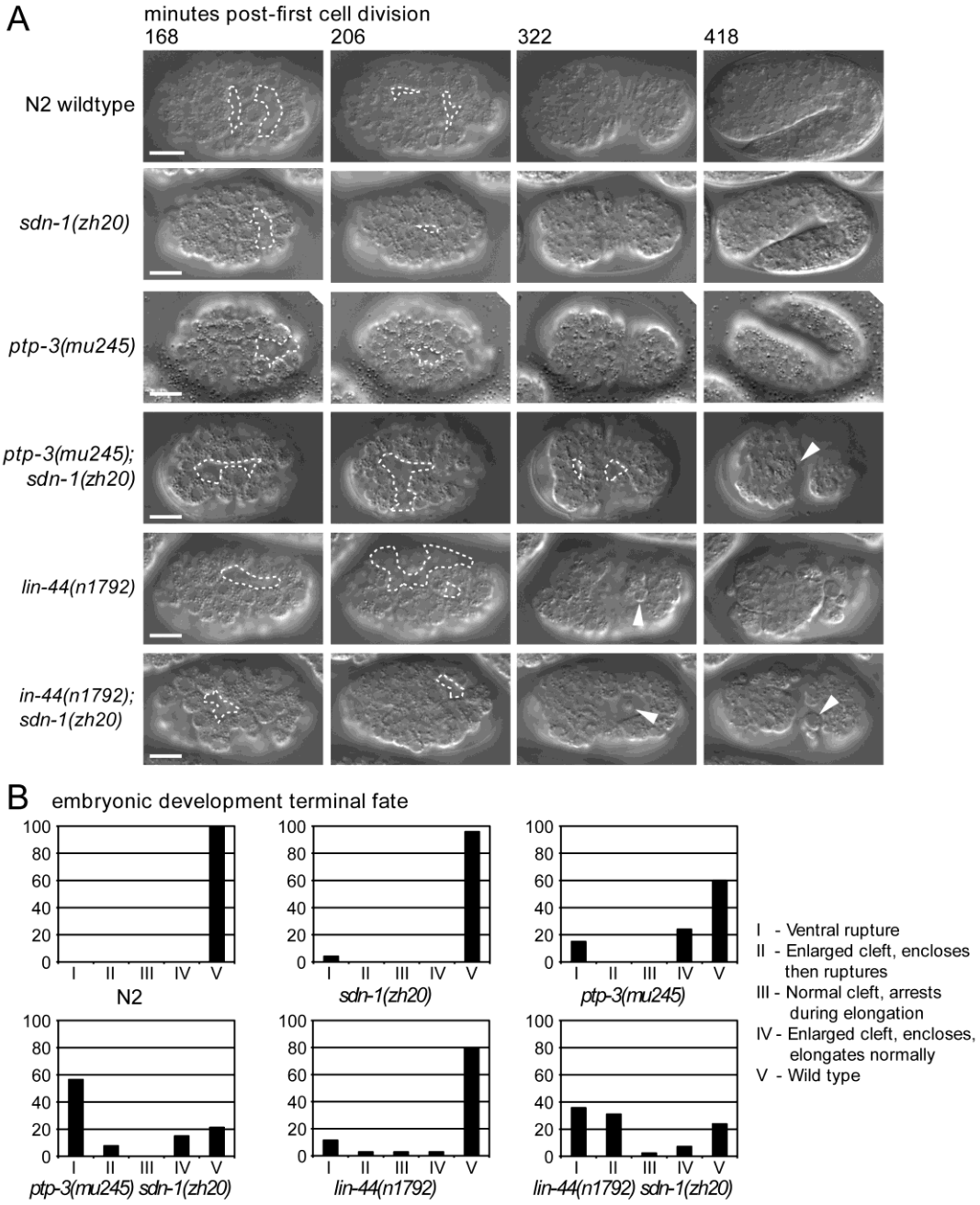
A
minutes post-first cell division
168
206
322
418
N2 wildtype
sdn-1(zh20)
ptp-3(mu245)
ptp-3(mu245); sdn-1(zh20)
lin-44(n1792)
in-44(n1792); sdn-1(zh20)
B
embryonic development terminal fate
100
80
60
40
20
0
I II III IV V
N2
sdn-1(zh20)
ptp-3(mu245)
ptp-3(mu245) sdn-1(zh20)
lin-44(n1792)
lin-44(n1792) sdn-1(zh20)
I - Ventral rupture
II - Enlarged cleft, encloses then ruptures
III - Normal cleft, arrests during elongation
IV - Enlarged cleft, encloses, elongates normally
V - Wild type

Figure 2.3 The dual loss of *ptp-3* and *sdn-1* results in synergistic defects during embryogenesis (A) Using 4D time-lapse microscopy we monitored embryogenesis in N2 wild-type, *ptp-3, sdn-1, lin-44* single mutants, and *lin-44; sdn-1* and *ptp-3; sdn-1* double mutants. The gastrulation clefts (outlined regions) present in the single mutants are more likely to close during development than the clefts in the double mutants. The arrowhead indicates cells that have extruded from the internal region of the embryo through the open gastrulation cleft (panel 418 minutes). (B) Terminal fates of the embryos plotted by genotype. (Image acquisition and analysis done by Dr. Martin Hudson.)

Figure 2.4

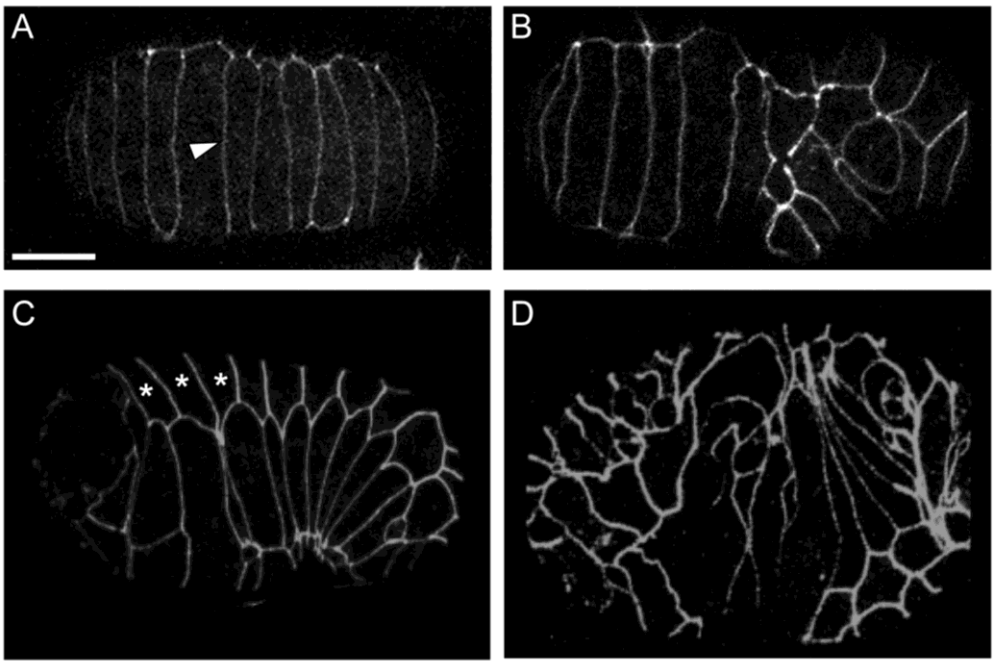

Figure 2.4 Epidermal junctions can be maintained in cell-adhesion mutants and RNAi treated animals We used an AJM-1::GFP transgene (*jcIs1)* to examine epidermal morphology in animals being tested. (A) In wild-type *jcIs1* animals, AJM-1::GFP is localized to cell junctions (arrow) and outlines epidermal cells. Here a view of the dorsal epidermal cells is visible. (B) A dorsal view of an *sdn-1(zh20)* animal showing disorganized epidermal cells in the posterior half of the embryo. (C) Ventro-lateral view of a wild-type embryo just after ventral enclosure. Asterisks mark the hexagon-shaped lateral seam cells. Note the regular morphology. (D) A *sdn-1(zh20)* animal treated with *lin-44 RNAi.* While some lateral seam cells (asterisks) are correctly. (Experiments and analysis were carried out by Curtis Yingling and Samantha N. Hartin.)

Figure 2.5

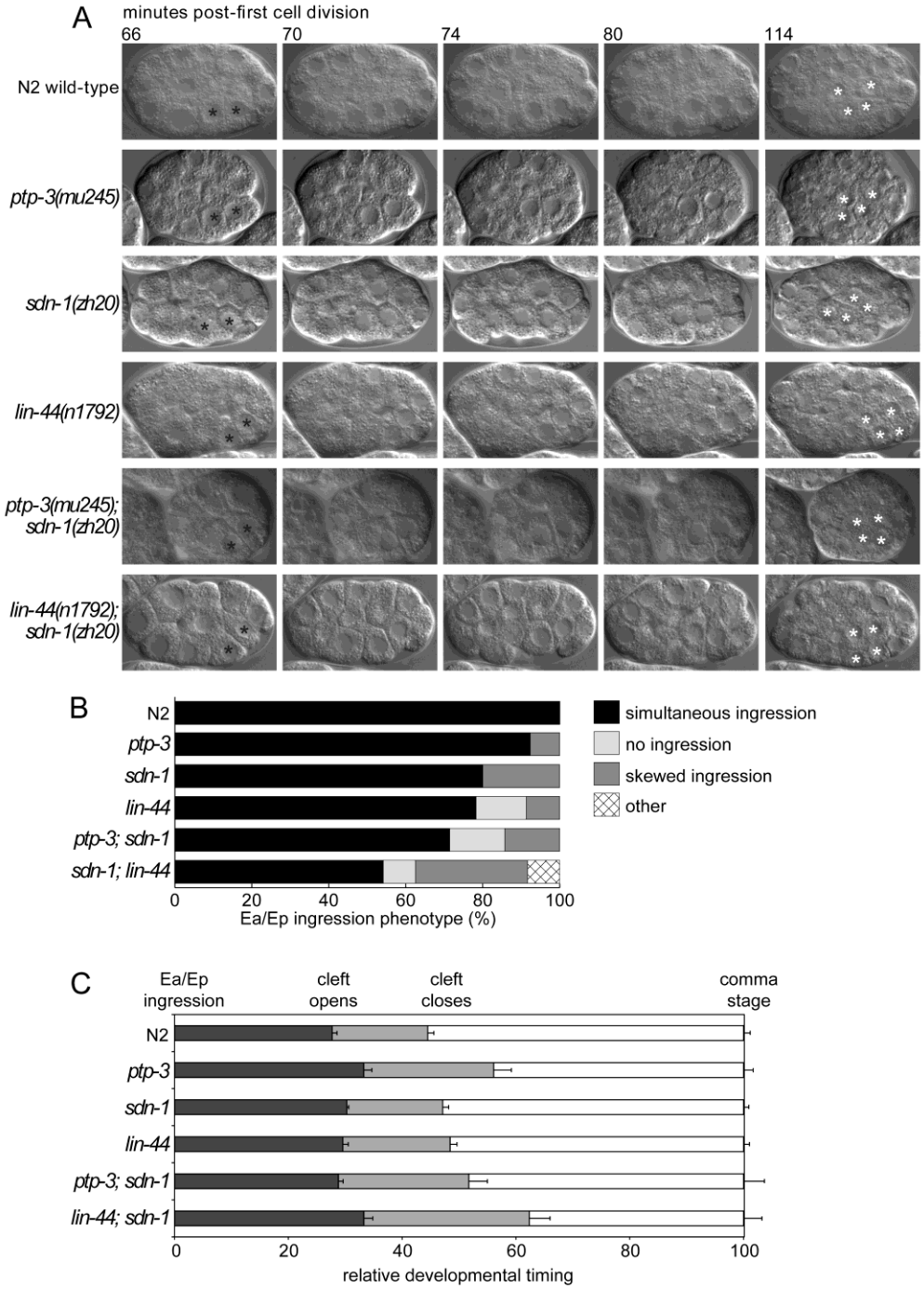
A
minutes post-first cell division
66
70
74
80
114
N2 wild-type
ptp-3(mu245)
sdn-1(zh20)
lin-44(n1792)
ptp-3(mu245); sdn-1(zh20)
lin-44(n1792); sdn-1(zh20)
B
N2
ptp-3
sdn-1
lin-44
ptp-3; sdn-1
sdn-1; lin-44
simultaneous ingression
no ingression
skewed ingression
other
0
20
40
60
80
100
Ea/Ep ingression phenotype (%)
C
Ea/Ep ingression
cleft opens
cleft closes
comma stage
N2
ptp-3
sdn-1
lin-44
ptp-3; sdn-1
lin-44; sdn-1
0
20
40
60
80
100
relative developmental timing

Figure 2.5 *sdn-1* mutations enhance *lin-44* gastrulation defects. (A) In *C. elegans*, gastrulation is initiated by the inward migration of the endodermal precursor cells Ea and Ep (black asterisks). In *sdn-1* and *ptp-3* mutant animals, the cells ingress, become completely surrounded by neighboring cells, then divide laterally (white asterisks). Note that Ea and Ep are completely internalized prior to the lateral cell division. In *lin-44* and *sdn-1* mutants, Ea/Ep ingression is often asynchronous. In addition, some *lin-44* embryos show a more severe phenotype, where the Ea/Ep cells completely fail to ingress. The subsequent lateral cell division positions two of the daughter cells onto the surface of the embryo, generating a "Gut on the exterior", or Gex phenotype [77]. Similar but more penetrant defects are observed in *lin-44; sdn-1* double mutants. (B) Summary of Ea and Ep cell ingression behavior by genotype. The *lin-44; sdn-1* double mutants exhibit a higher rate of Ea and Ep ingression defects than either single mutant. (C) Relative timing of developmental milestones as a function of genotype. Note the *lin-44; sdn-1* double mutants have a significantly longer period in which the gastrulation cleft is open. (Image acquisition and analysis done by Dr. Martin Hudson.)

Section 2.7 Tables

Table 2.1 Lethality by genotype analyses

Genotype [a]	Brood Size Avg (St Dev) [b]	Phenotype [c] Avg (St Dev)				N [d]
		Emb	Lva	Vab	WT	
wild type	247.6 (35.6)	0.5 (0.6)	1.0 (0.7)	0.0 (0.0)	98.5 (0.9)	1238
ptp-3(mu245)	82.0 (51.6)	2.1 (1.7)	8.4 (4.7)	2.2 (2.8)	87.3 (7.2)	984
sdn-1(zh20)	173.6 (101.0)	7.7 (5.3)	5.5 (3.7)	0.6 (0.7)	86.6 (6.1)	868
ptp-3(mu245)/mIn1mIs14; sdn-1(zh20)	114.2 (35.7)	8.2 (2.6)	9.6 (1.8)	1.8 (2.4)	80.4 (4.2)	1142
ptp-3(mu245); sdn-1(zh20)	10.2 (6.7)	84.3 (8.4) †	15.7 (4.1) †	0.0 (0.0)	0.0 (0.0) †	51
lin-44(n1792)	137.4 (33.9)	12.2 (2.9)	10.6 (2.1)	0.4 (0.6)	76.8 (3.4)	687
sdn-1(zh20); lin-44(n1792)	94.8 (38.4)	71.6 (11.0) †‡	4.6 (1.9)	0.4 (0.9)	23.5 (12.0) †‡	474
sdn-1(zh20); lin-17(n671)	76.6 (12.6)	4.4 (8.0)	1.3 (1.1)	0.0 (0.0)	93.6 (7.8)	383
ptp-3(mu245); lin-44(n1792)	101.2 (49.0)	4.6 (3.2) ‡	21.5 (5.7) ‡	1.3 (1.3)	68.7 (8.7) ‡	506

[a] Listed genotype is the maternal genotype
[b] average total brood size of five mothers
[c] percent of animals displaying phenotype from mothers of indicated genotype
[d] total number of offspring analyzed
† Significantly different from *sdn-1(zh20)* p<0.01 (Students t-test)
‡ Significantly different from *lin-44(n1792)* p<0.01 (Students t-test)

Table 2.2 SynLet Genes by Genotype Affected

WormBase Identification	Overlapping CDS(s)	Gene Name	Description
SynLet with ptp-3			
WBGene00006776	T19B4.7	*unc-40*	Netrin receptor
WBGene00007301	C04F12.7		Multiple transmembrane domains
WBGene00007768	C27C7.5		Carbohydrate binding domain protein
WBGene00023237	C17C3.14		Psuedogene
WBGene00006868	M03A1.1	*vab-1*	Ephrin receptor tyrosine kinase
WBGene00016638 [a]	C44B12.5	*perm-4*	Secreted protein
WBGene00022539 [a]	ZC190.5		Multiple transmembrane domains
SynLet with *sdn-1*			
WBGene00007900	C33D9.6		Coiled coil domains
WBGene00015009	B0041.5		Solute carrier family 35-like
WBGene00016753	C48E7.8	*oac-9*	O-acyltransferase
WBGene00008411	D2030.1	*mans-1*	Mannosidase
WBGene00000254	K04F10.4	*bli-4*	KEX2/subtilisin-like serine endoprotease
WBGene00020397	T10B11.1	*pcbd-1*	pterin-4-α-carbinolamine dehydratase
WBGene00009666	F43G9.3		Secreted protein
WBGene00006061	F30A10.5	*stl-1*	Stomatin-like
WBGene00011783	T15D6.9		Secreted protein
WBGene00016253	C30E1.4		Secreted protein
WBGene00003029 [b]	E01A2.3	*lin-44*	Wnt ligand
SynLet with *ptp-3* and *sdn-1*			
WBGene00000253	F56C11.1	*bli-3*	Dual oxidase
WBGene00003569	F35C12.2	*ncx-4*	Na^+/Ca^{2+} exchanger
WBGene00008294	C54C8.7	*clec-11*	C-type lectin
WBGene00003186	Y54E10BL.6	*mek-2*	MAP kinase kinase
wt Let, but not in *ptp-3* or *sdn-1*			
WBGene00044058	F17B5.6		Carbohydrate transferase
WBGene00007139	B0285.7	*mnp-1*	Matrix non-peptidase
WBGene00007666	C18B12.4		Plasma membrane-associated ring-finger domain containing protein

[a] Let phenotype observed in wild-type also, but not in *sdn-1*
[b] Let phenotype observed in wild-type also, but not in *ptp-3*

Table 2.3 AJM-1::GFP analysis by genotype

		wild-type			*ptp-3*			*sdn-1*		
Class	RNAi	Normal	Defective	% Defective	Normal	Defective	% Defective	Normal	Defective	% Defective
Control	vector	108	0	0%	100	4	4%	13	87	87%
***sdn-1* SynLet**	*bli-4*	94	6	6%	12	76	86%	N/D		
***sdn-1* SynLet**	*lin-44*	42	81	66%	7	90	93%	N/D		
***sdn-1* SynLet**	*oac-9*	22	82	79%	8	93	92%	N/D		
***ptp-3* SynLet**	*unc-40*	92	6	6%	4	96	96%	3	99	97%
***ptp-3* SynLet**	*vab-1*	35	82	70%	N/D			2	100	98%
***sdn-1* & *ptp-3* SynLet**	*ncx-4*	94	6	6%	2	98	98%	6	79	93%
Other	*mnp-1*	29	75	72%	0	100	100%	11	91	89%

N/D not determined

Chapter III

C. elegans sdn-1 modulates Wnt signaling to ensure proper axon outgrowth and termination in motorneurons

Section 3.1 Abstract

Heparan sulfate proteoglycans (HSPGs), such as syndecan, regulate many aspects of neural development including cell migration, axon guidance and synapse formation. HSPGs have also been shown to be important modulators of extracellular growth factors including Wnts. Wnts are among the long and short range signaling molecules that contribute to the formation and patterning of complex body structures like the nervous system. However, many questions remain about how HSPGs and Wnts interact *in vivo*.

The nervous system of *C. elegans* has a well-defined, stereotyped pattern of axon outgrowth, including the positions where axon growth is terminated. Previous work has shown that loss-of-function (LOF) in either *lin-44* or *egl-20* Wnt ligands results in an over-extension of the DD6 and/or VD13 axon into the posterior region of the animal where the Wnt ligands are expressed, consistent with the Wnts acting as repulsive cues. *lin-44;egl-20* double mutants have a more significant over-extension phenotype suggesting partial redundancy between these ligands.

We have identified genetic interactions between *sdn-1*, the *C. elegans* syndecan HSPG, and the *lin-44* and *egl-20* Wnt ligands. In *sdn-1* null mutants the posterior growing DD6/VD13 axons exhibit both under-extension and over-extension phenotypes. Unlike the Wnt ligand single mutants, which have only over-extended axons, the *lin-44;sdn-1 and egl-20;sdn-1* double mutants exhibit both under- and over-extension of these axons.

We propose a two-step model in which SDN-1 interacts with LIN-44 and EGL-20 for proper axon outgrowth and termination. We hypothesize that SDN-1 controls

Wnt signaling non-autonomously during axon outgrowth and then autonomously for proper axon termination. Understanding how SDN-1 interacts with these Wnt ligands will provide a better mechanistic view of the relationships that exist between HSPGs and Wnt growth factors.

Section 3.2 Introduction

The development of the nervous system is a highly ordered and complex process that requires multiple molecular cues to form functional circuits. During development axonal growth cones are guided to their correct position by external cues presented in the extracellular matrix (ECM). The nematode *C. elegans* provides a valuable model in which to study nervous system development. There are a plethora of genetic tools that can be used in *C. elegans* including but not limited to, chromosomal balancers, gene knock-outs, transgenic manipulations and fluorescent reporter proteins. *C. elegans* have 959 somatic cells of which, 302 are neurons that can be visualized *in vivo* with fluorescently labeled proteins. During the L1 larval stage the DD motorneurons are born along the ventral nerve cord and extend an axon anteriorly, which then bifurcates and sends a process dorsally. When the process reaches the dorsal nerve cord it bifurcates a second time and grows anteriorly and posteriorly. During late the L1/early L2 stage the VD motorneurons develop in the same manner, fasiculating with the DD motorneurons in along the nerve cords to form bundles. The growth and termination of these GABAergic motorneurons has been long studied in *C. elegans* with multiple molecules being implicated [26, 37, 124, 125].

Heparan sulfate proteoglycans (HSPGs) have been shown to act as modulators of signals that are crucial for proper axon guidance [15, 17, 62, 126-129]. HSPGs are present in the ECM as secreted proteins or are bound to the cell membrane. The extracellular domain is decorated with heparan sulfate side chains [17, 62, 130]. The individual sugars on these side chains are modified by

sulfotransferases and an epimerase before being transported to the cell membrane [47, 131]. These side chains bind multiple signaling molecules such as Wnts, and BMPs (Bone morphogenetic proteins), and can also act as co-receptors for other components of the ECM [34, 48, 60, 88, 129, 132, 133]. One of the major families of HSPGs are syndecans. These HSPGs not only have HS side chains but also feature an intracellular domain that contains a PDZ-like motif, suggesting that syndecans can also link to cytoplasmic signaling [134].

Most mammalian genomes encode for four syndecan proteins, while the *C. elegans* genome only encodes one, named *sdn-1*. In *C. elegans*, SDN-1 functions autonomously in the Hermaphrodite Specific Neurons (HSNs) to control cell migration and axon outgrowth, and in DDs and VDs to guide commissure growth along the dorsal-ventral axis [15]. SDN-1 has also been shown to regulate the guidance of non-neural tissues including the distal tip cells (DTC) that migrate along the anterior-posterior axis to form the gonad during larval development [31].

DTC guidance by SDN-1 is also mediated by the Wnt ligand, EGL-20, and recent reports have demonstrated genetic interactions between SDN-1 and Wnt ligands [30, 31, 113]. In early embryogenesis SDN-1 functions in a MOM-2/Wnt-dependent signaling event to direct cell specification [30]. We previously demonstrated that *sdn-1* and *lin-44* function in genetically-redundant pathways during gastrulation. Together these data indicate that SDN-1 is likely to function in Wnt growth factor signaling in *C. elegans* as has been demonstrated in vertebrates.

Here we show that SDN-1 along with three of the five *C. elegans* Wnts work in a combinatorial manner to control the termination of GABAergic motor neurons

within the dorsal nerve cord along the anterior-posterior body axis. Rescue experiments suggest the effects of SDN-1 on axon termination were both cell-autonomous and non-autonomous. Additional epistasis experiments suggested that *sdn-1* was genetically downstream of Wnt ligands, but upstream of Wnt effectors, *e.g.* Dishevelled or β-catenin. Similar results have previously been demonstrated in Wnt signaling for the CAM-1/Ror tyrosine kinase [135-141]. Our results suggested that SDN-1 is likely to be functioning in a co-receptor or Wnt patterning role to regulate D-type neuron axon termination in the dorsal nerve cord.

Section 3.3 Results

Syndecan is an anterior/posterior axon guidance factor

The GABAergic D-type motorneuron cell bodies are located along the VNC. The six DD and thirteen VD cell bodies extend a neuronal process anteriorly, bifurcates and send a process dorsally, then bifurcates again at the DNC and sends a process anteriorly and posteriorly. In the DNC, the DD processes fasciculate with those of the VD neurons and terminate at stereotyped positions along the anterior-posterior axis [25]. The most posterior DD and VD processes extend as a bundle that terminates at the anterior-posterior position superior to the locations of the DD6 and VD13 cell bodies, which are located on the ventral side[40](Figure 3.1). It is this stereotyped development that allows for easy detection of aberrant axon outgrowth.

We observed that *sdn-1(zh20)* mutants had defects in the termination point of the GABAergic axons in the dorsal nerve cord (DNC), similar to what was previously characterized by Maro, Klassen et al., 2009. We found that in 39.5% of *sdn-1(zh20)* mutants (a *sdn-1* null allele) the D-type axons failed to reach the correct termination point, and that in 51% of *sdn-1(zh20)* mutants the axons extended further into the tail (posteriorly) when compared to wild-type animals (Figure 3.2). We also tested a second LOF allele, *sdn-1(ok449)* which results in an in-frame deletion that produces a truncated form of SDN-1. This shortened form lacks two of the major conserved heparan sulfate attachment sites in the extracellular domain [99]. We found that animals with the *ok449* mutation had similar defects to those found with the *zh20* allele. The remainder of our study was conducted using the

zh20 allele since that has been demonstrated to be a genetic and molecular null [15, 30].

The VD neurons are formed at the end of the first larval stage (L1) and finish their initial outgrowth during the beginning of the second larval stage (L2). We initially scored animals in the fourth larval stage (L4). Between the L2 and L4 stages animals approximately double in length. To determine if *sdn-1* axon outgrowth errors were due to developmental failures or a failure to keep up with the growth of the animal we scored DNC termination in *zh20* animals at the L2 stage. We found that like those scored at later stages, *zh20* animals at the L2 stage had both over- and under-extended GABAergic axons in the DNC, suggesting that the initial formation of the GABAergic axons is defective, although we cannot completely rule out a secondary role whereby SDN-1 also ensures allometric axon growth with body length. It is worth noting that in other genetic contexts where D-axon termination has been investigated, it is common to observe both under- and over-extension defects in the same genotypes [40, 142].

To determine if the effects of axon guidance along the anterior-posterior axis were limited to the D-type neurons we examined the axons of the six mechanosensory neurons using an integrated GFP reporter, *muIs32.* In wild-type animals the Anterior Lateral Mechanosensory (ALMs) and the Posterior Lateral Mechanosensory (PLMs) neurons extend anteriorly-directed axons from their cell bodies and have a characteristic termination point, with the PLMs terminating just posterior to the ALM cell bodies and the ALMs terminating just posterior to the nose

of the animal (Figure 3.3). In addition, the axons are largely parallel to the dorsal and/or ventral nerve cords, and do not appear to deviate in the dorsal-ventral axis, except where they make branches into the ventral nerve cord (PLMs) or the nerve ring (ALMs).

When we examined the ALM and PLM neurons in *sdn-1(zh20)* mutant animals we found significant disruptions in the outgrowth of theses neurons. As had been previously reported the ALM cell bodies were frequently displaced posteriorly, likely due to incomplete cell migration. As such we did not further examine axon outgrowth errors in the ALM axons. The PLM neurons do not undergo long-range cell migrations, and the cell bodies were in grossly normal positions in *zh20* mutants. We found that PLM axons frequently terminated prematurely, but also showed evidence of failure to terminate growth, and could "hook" toward the ventral nerve cord [37, 142] We also observed defects in the outgrowth of the AVM and PVM axons. In wild-type animals, the AVM and PVM axons grow towards the ventral midline before turning anteriorly. In *sdn-1(zh20)* mutants we observed some AVM and PVM axons that were first directed anteriorly prior to making a ventral turn (Figure 3.3). Together with previously published results and our data for the D-type neurons we conclude that SDN-1 is a determinant of anterior-posterior axon guidance and termination in *C. elegans.*

Syndecan function is required in multiple tissues to regulate D-type neuron outgrowth

We were able to partially rescue the outgrowth phenotypes associated with the *zh20* lesion by reintroducing SDN-1. We obtained a Mos1 single copy insertion (Mos-SCI), *juSi119,* in which a GFP-tagged version of SDN-1 under the regulation of endogenous *sdn-1* promoter elements had been inserted on the second chromosome (LG II) (Figure 3.4). The *zh20;juSi119* animals had no undergrowth in the DNC (6% vs. 39.5% in *zh20*, P<0.0001), but still had a high rate of DNC overgrowth (56%). To determine if this was due to the GFP insertion we obtained a second Mos-SCI, wpSi12, which is inserted in the same chromosomal position, but is not GFP tagged. We observed equivalent rescue of the under-extension phenotype (1% vs. 39.5% in *zh20*, P<0.0001). We generated *zh20* homozygotes in which *juSi119* was heterozygous (*zh20;juSi119/+*) and found no change in the ability of the transgene to rescue the under-extension phenotype (36% vs 39.5% in *zh20*), but a partial rescue of the over-extension phenotype (22% vs. 51% in *zh20*). Thus we are able to rescue both aspects of the outgrowth phenotype, both under- and over-extension of the GABAergic axons in the DNC, by endogenous *sdn-1* expression (Figure 3.4).

To test whether *sdn-1* could be functioning cell-autonomously we drove the expression of *sdn-1* specifically in the GABAergic neurons using the *unc-25* promoter (injected at 1 ng/µl). We found that when we cell-specifically expressed *sdn-1* we were able to partially rescue the over-extension phenotype in *zh20* (21% vs. 51%, P<0.0001), but the rate of under-extended axons was unchanged (30% vs. 39.5%).

We generated a second transgene at a higher concentration (5 ng/µl) and found no differences in rescue. We were still unable to rescue the under-extension defects (34% vs 39.5) and there was no increase in the efficiency of rescuing the over-extension defects (19% vs. 51%) (Figure 3.4). However, at the higher concentration we did observe an increase in the axon guidance defects in other aspects of outgrowth suggesting we were likely to be reaching an over-expression effect. These data suggest that the over-extension of axons is due, at least in part, to the cell-autonomous loss of *sdn-1*, and that the under-extension likely requires *sdn-1* function in other tissues.

The SDN-1::GFP expressed by *juSi119* is present broadly throughout the animal, including in the DNC and tissues surrounding it, including the muscle, epidermis and intestinal cells in the posterior of the animal. We further examined whether SDN-1 was expressed in the D-type neurons using a cytoplasmic RFP (*Punc-25::mCherry*). In L1 animals, after DD neurons have formed, but prior to the formation of the VD neurons, SDN-1GFP was present in the nervous system, but we found no evidence of expression in the D-neurons. However, later in development, after the VD neurons have formed, SDN-1::GFP was clearly being expressed in the GABAergic motorneurons. This is consistent with a model whereby SDN-1 functions early to promote axon outgrowth non-autonomously, but functions, cell autonomously later in development to restrict growth.

sdn-1 is required for Wnt-dependent axon outgrowth and termination

Previous work has demonstrated that Wnt signaling can regulate axon termination of the D-type neurons [40]. Consistent with those observations we also found that animals with mutations in the most posteriorly expressed Wnt ligand, *lin-44(n1792)*, caused the DNC axons to over-extend in 97% of animals (Figure 3.5). Previously we have found that *sdn-1* and *lin-44* exhibit a synthetic lethal genetic interaction in early development, with ~75% of double mutants dying during embryogenesis [41]. To determine whether *sdn-1* was functioning in *lin-44* dependent outgrowth we generated double mutants. We were able to score the axons in the surviving animals, and found that they exhibited both under and over-extended DNCs that were not significantly different from *sdn-1* single mutants (P<.3, N=200).

Another Wnt ligand, *egl-20,* has also been found to affect DNC termination. We obtained two putative null alleles of *egl-20*, *lq42* (pers. comm. Erik A Lundquist) and *gk453010* from the Million Mutation Project [143]. Both *lq42* and *gk453010* create premature stop codons in the *egl-20* mRNA, unlike the reference allele, *n585*, which is a missense mutation. We found that in both *egl-20(lq42)* and *egl-20(gk453010)* the DNC axons over-extended into the posterior in about 69% of the animals (Figure 3.5). Qualitatively, we observed that the extent to which the axons extended past the expected termination point was lower in *egl-20* mutants than in *lin-44* mutants.

We generated *lin-44; egl-20* double mutants, and found that DNC axons extended past the wild-type termination point, and that consistent with previous reports, the axons grew further posteriorly than in either single mutant. However, we also observed that complete loss of both Wnt ligands also resulted in axons of the DNC appearing to be under-extended, terminating prior to the expected position (Figure 3.5). These results suggest there are two Wnt-mediated events in the growth of the GABAergic neurons in the DNC. First, a growth promoting function, which ensures that axons grow from the commissure to the normal termination point, and second, growth restricting function, which prevents axons from extending past the normal termination point.

Based on our results from the *zh20* rescue we inferred that the mechanisms of SDN-1-dependent axon extension from the commissure to the normal termination point is distinct from those that prevent the axon from growing past the termination point. The former appears to be a cell non-autonomous function of SDN-1, while the latter appears to be at least partially cell-autonomous for the GABAergic neurons. Thus, to simplify the analysis we first focused on the combined role of Wnts and SDN-1 on the outgrowth of axons from the commissure to the normal termination point, failures in which caused the DNC to appear under-extended.

sdn-1 functions in a Wnt signaling pathway to promote axon extension

We found that the rate of axon under-extension was equivalent in the *sdn-1* single mutants to the *lin-44; egl-20* double mutants. These data argue that the Wnt ligands are both partially redundant and promote axon outgrowth from the

commissure. Wnt signaling has been well studied, and in a canonical signaling pathway, activation of Frizzled receptors by Wnt ligands activates the cytosolic protein Dishevelled. Dishevelled then inhibits the GSK3, Axin, APC destruction complex. This inhibition allows β-catenin to activate the transcription of target genes with the help of TCF-LEF transcription factors [144].

Consistent with Wnt signaling being both growth promoting and restricting, we found that mutations in other Wnt signaling components, including *lin-17/*Frizzled (24%) and *mig-5/*Dishevelled (44%) can result in under-extension of the DNC, as had been reported [40]. We created double mutants of *sdn-1* with *lin-17* and *mig-5* and found these animals exhibited under-extension (*lin-17; sdn-1* – 31% (P = 0.08), *mig-5; sdn-1* – 44% (P >0.05)) that were not significantly different from the single mutants. In contrast, the loss of *bar-1/*β-catenin, results in a highly penetrant under-extension phenotype (96% - our observations); [40]). Removing *sdn-1* from *bar-1* mutants had no effect on axon growth as 95% of the double mutants exhibited an under-extension phenotype. From these we conclude that for axon extension *sdn-1* is functioning in the Wnt pathway at a level equivalent with the Frizzled and Dishevelled proteins, upstream of β-catenin.

Since loss of *lin-44; egl-20* resulted in only a 45% under-extension phenotype we asked whether a third Wnt ligand, *mom-2*, could also function in this pathway. The *mom-2* gene is expressed in the L1 stage, in the posterior of the animal near the region where the DNC is forming. We examined *mom-2(or77)* mutants and found no evidence of under-extension in the DNC, although we did see over-extension (see

below). Double mutants of *mom-2* with *lin-44* (0%) and *egl-20* (3%) did not result in under-extension defects. Triple mutants were sick and difficult to obtain, so we used RNAi to knockdown *mom-2* in *lin-44; egl-20* double mutants. Although *mom-2* RNAi caused a highly penetrant embryonic lethality we were able to obtain sufficient numbers of escapers to analyze the DNCs. Compared to the double mutants alone we actually observed a decrease in the rate of under-extension (9% vs. 46.5% in *lin-44;egl-20*) in escapers. Thus, it is unlikely that MOM-2 is functioning redundantly with LIN-44 and EGL-20 to activate BAR-1 to promote axon extension from the commissure to the termination point.

sdn-1 functions in a Wnt signaling pathway to inhibit axon extension

Interestingly, loss of function in *sdn-1* and Wnt signaling genes, with the exception of *bar-1,* also result in axons that grow past the normal termination. A necessary first step in the DNCs being able to be over-extended could be that they reach the wild-type termination point. Thus, to evaluate over-extension we counted the DNCs that were extended past the normal termination point as a fraction of those that were not under-extended. Thus, in *sdn-1* mutants 51% of all animals had over-extended DNC, but when we removed animals with under-extension defects we found that 84% of axons that reached the wild-type termination point were over-extended. When we removed either *lin-44* or *egl-20* or both from *sdn-1* animals we observed similar rates of over-extension (*lin-44;egl-20* – 46.5% (P=.42 vs *sdn-1*) *lin-44; sdn-1* – 58.5% (P>.29 vs *sdn-1*), *egl-20; sdn-1* – 66% (P>0.003 vs *sdn-1*), *lin-44; egl-20; sdn-1* – 67% (P>0.002 vs *sdn-1*)). These suggest that the Wnt ligands and

SDN-1 are in the same pathway to promote axon termination at the wild-type position.

We subsequently examined over-extension in the *lin-17/*Frizzled and *mig-5/*Dishevelled mutants. The *lin-17* mutants had an over-extension phenotype in 56% of animals, and removal of *sdn-1* in that background resulted in over-extension 47.7% of the time (P=0.1143 vs *lin-17*, P=0.5394 vs *sdn-1*). When corrected for multiple tests, we concluded that there is no significant difference between the double mutants and either single mutants. For *mig-5* we observed over-extension in 46% of single mutants and in 35.6% of animals lacking both *mig-5* and *sdn-1* (P=0.1178 vs *mig-5,* P=0.004 vs *sdn-1*). The penetrance of these is suggestive that *mig-5* is required for *sdn-1* mutants to be over-extended, likely placing it downstream of *sdn-1.*

HS modifications are important for SDN-1 to interact with LIN-44 and EGL-20 in a context dependent manner.

The glycosaminoglycan side chains on SDN-1 are modified by two sulfotransferases, HST-2 and HST-6 and an epimerase, HSE-5 [62, 145]. Each enzyme has been shown to be involved in multiple aspects of neural development through the specific modifications each makes [15, 17, 47, 127]. We examined the loss of function mutation for each of the modifying enzymes to determine which heparan sulfate sugar modifications are important for the interaction between SDN-1, LIN-44 and EGL-20. We found that all three enzymes are need for both processes (Figure 3.8).

HSE-5 is a C5-epimerase that is predicted to catalyze the chain-modifying epimerization of glucuronic acid to iduronic acid during heparan sulfate biosynthesis. HSE-5 is expressed in the hypodermis and intestine [47]. Previously, HSE-5 has been shown to function in parallel to SDN-1 for D-type motorneuron dorsally directed commissure outgrowth and VNC fasciculation [15]. We found that *hse-5* LOF significantly decreased the penetrance of over-extension seen in *sdn-1* (29% *lin-17* vs. 51% *sdn-1,* P<.0001) but did not significantly change the penetrance of under-extension defects (43.5% *lin-17* vs. 35.5% *sdn-1*) (Figure 3.8). Suggesting that another proteoglycan that is modified by *hse-5* is involved in the termination process and can partially compensate for the loss of *sdn-1*. These data also suggest the initial modification of SDN-1 by HSE-5 may be important for axon outgrowth. When mutated with *lin-44*, *hse-5* did not significantly enhance the penetrance of under-extension seen in *lin-44;sdn-1* double mutants (37% *lin-44;hse-5* vs. 34% *lin-44;sdn-1*, P= .06) suggesting HSE-5 is important for the interaction between SDN-1 and LIN-44 during axon outgrowth. When both *hse-5* and *egl-20* are mutated together the penetrance of over-extension is not significantly different from *egl-20* alone. Loss of *hse-5* and *egl-20* is not significantly different than the loss of *egl-20* and *sdn-1* (62%-over, 7%-under *egl-20;hse-5* vs. 66%-over, 14%-under *egl-20;sdn-1*), suggesting *egl-20* interacts with the side chains of *sdn-1* during both processes.

Two heparan sulfotransferases *hst-2* and *hst-6* are needed to modify syndecan side chains after *hse-5*. During neuronal development *hst-6* is expressed in neuronal tissues and *hst-2* is expressed in the hypodermis [47]. When mutated alone both show a lower penetrance of under-extension defects that of *sdn-1*

mutants (23% *hst-2* and 13% *hst-6*) (Figure 3.8). Loss of either *hst-2* or *hst-6* with *lin-44* does not recapitulate the under-extension phenotypes seen in *lin-44;sdn-1* (11% and 0% respectively vs. 34% *lin-44;sdn-1)* suggesting other modifying enzymes and/or other molecules play a role during axon outgrowth (Figure 3.8). Interestingly, the penetrance of under-extension seen in *egl-20;hst-2* was not significantly different from *egl-20;sdn-1* (16.5% *egl-20;hst-2* vs. 14% *egl-20;sdn-1*).

Over-extension defects seen in *hst-2* or *hst-6* are not significantly different than *sdn-1* (46% *hst-2* and 55% *hst-6*) suggesting they are important for axon termination. Loss of *lin-44* with *hst-2* is significantly different than *lin-44;sdn-1* (78.5% vs 58%). This increase suggests that *hst-2* could be functioning in a parallel pathway. In fact, when we tested the LOF in both *hst-2* and *egl-20* we discovered that the loss of both is not significantly different that the loss of both *egl-20* and *sdn-1* (57% vs. 66%). Loss of *hst-6* also showed similar results with *egl-20* (72% vs.66%). However, loss of *hst-6* and *lin-44* did not recapitulate the phenotype seen in *lin-44;sdn-1* (97.5% vs 58%) but was more similar to the loss of *lin-44* alone (97.5% double vs. 97% *lin-44*).

Taken together these data suggest that different modifications of the SDN-1 side chains function in a combinatorial fashion with either LIN-44, EGL-20 and some yet unidentified molecule during axon outgrowth and termination.

Section 3.4 Discussion

During nervous system formation multiple molecular cues provide instructive signals that guide axons to their destinations. Here we demonstrated that the single *C. elegans* syndecan protein functions as both a positive and negative regulator of axon outgrowth along the anterior-posterior axis. Syndecans have been implicated in growth factor signaling and demonstrated to function co-operatively with Frizzled receptors, however their role in Wnt-mediated axon guidance has not been specifically demonstrated. Here we find that loss of function in *sdn-1* is similar to the simultaneous loss of two Wnt ligands, *lin-44* and *egl-20,* suggesting *sdn-1* is a positive regulator of Wnt signaling. Consistent with that we find that *bar-1*/β-catenin is necessary for *sdn-1* mutants to display over-extension in the DNC, suggesting that SDN-1 is functioning via β-catenin.

SDN-1 functions in anterior-posterior axon outgrowth and termination.

In *C. elegans* the D-type neurons use self-avoidance to tile their axons along the anterior-posterior axis, but the most posterior cells (DD6, VD13) have no D-type neurons located to their posterior. Further, the dorsal nerve cord in *C. elegans* does not specifically terminate where the D-type neurons do, rather it is contiguous along the dorsal side of the animal, and thus these axons lack obvious landmarks to instruct them where to stop growing. Similarly, the PLM axons do not appear to have an obvious physical landmark (cell, axon, *etc.,* that instructs the axon where to terminate Loss of *sdn-1* function in *C. elegans* results in D-type motorneuron and

PLM axons that stop short of their normal termination point, as well as axons that extend past their normal termination point. We conclude that molecular cues, such as SDN-1 provide contextual information to stop axon growth at the appropriate position.

SDN-1 function has been investigated in D-type neurons previously [15]. Most germane to our data was a study when D-axons were severed by laser axonotomy. In that context, loss of *sdn-1* appeared to inhibit regeneration suggesting that SDN-1 can stabilize the growth cone of the regenerating axons. This would be consistent with our observation that axons in *sdn-1* mutants terminate prematurely. In the study of regenerating axons, *sdn-1(-)* axons had more periods of unproductive growth, where they did not extend toward the dorsal nerve cord [36]. Thus, if the same events occurred in the DNC during development we would expect axons to fail to reach the normal termination point. Since we found that the percentage of animals with premature termination points as the same in L2 animals as seen later in development, we would conclude that the deficit in extension likely occurred during the earliest stages of axon outgrowth.

SDN-1 functions both autonomously and non-autonomously in D-type motorneurons.

One question is how can SDN-1 both promote and inhibit axon outgrowth? Our results suggest that these functions are likely mediated by different cells expressing SDN-1. SDN-1 is expressed in multiple different tissues including the hypodermis and nervous system [15]. Previous work has suggested that axon

guidance by SDN-1 was largely non-autonomous, most likely from the hypodermal cells that form one of the growth substrates for the axons [36]. When we replaced SDN-1 function broadly in the animals we found that we could only rescue the under-extension of axons, but could partially rescue the under-extension when we decreased the levels of SDN-1 by making the integrated transgene heterozygous.

We were able to partially rescue the over-growth phenotype by specifically expressing SDN-1 in the D-type neurons. This suggests that SDN-1 can function cell-autonomously, and in the D-type neurons it functions to restrict outgrowth. Unlike constructs where SDN-1 was expressed using its endogenous promoter, we found that increasing the concentration of DNA in the transgenes resulted in defects in the axonal migration of the D-type neurons, with no appreciable increase in rescue of the termination phenotype in the DNC.

It is unclear why the integrated SDN-1 transgenes, being under the control of the endogenous promoter elements, could not fully rescue the axon outgrowth defects. However, it is worth noting that previous studies using SDN-1 integrants at this chromosomal location were unable to fully rescue an *sdn-1* loss-of-function phenotype [36]. It is possible that the integrations we are using are missing long-distance regulatory elements. Our heterozygous integrant rescue data suggest this is not the complete explanation. It is also possible that the integration position in the chromosome alters the levels of expression from the endogenous promoter. We do not see a pronounced dominant effect of the transgene on D-type neuron growth in wild-type animals, suggesting the overall levels of SDN-1 expression *in vivo* are tightly regulated.

The SDN-1::GFP protein is present in the animals very early in development, with broad tissue distribution. We also observed an aggregation of SDN-1::GFP near the termination point of the D-type neurons in the DNC, although the axons do not appear to specifically terminate at this position, rather they extend a short distance past the point where SDN-1 was concentrated. Based on its colocalization with a marker specific for the D-type axons, we infer that the SDN-1::GFP is present in those cells, although the focused concentration we observe may not be limited to the D-neuron process. Similarly we find LIN-17 to be concentrated near the normal termination point of the D-axon, consistent with previous results [40]. We found that the foci of LIN-17 and SDN-1 are coincident near the termination point of the D-axons.

Syndecans are known to regulate the local concentration of Wnt ligands, and in *C. elegans,* loss of *sdn-1* results in the diffusion of EGL-20 away from source cells [31]. Thus, one possibility is that SDN-1 is acting to promote Wnt signaling, likely via LIN-17, at the termination point of the D-type neurons, to inhibit outgrowth. These results are consistent with our genetic data in that the loss of *sdn-1* and *lin-17* are both associated with outgrowth errors.

Heparan sulfate modification of SDN-1 is partially required for function

SDN-1 is decorated with heparan sulfate and chondroitin sulfate side chains that are modified by such enzymes has HSE-5, HST-2 and HST-6**.** Our results suggest that specific sugar modifications on the side chains of SDN-1 regulate different ligand interactions during axon outgrowth and termination separately. This type of

side chain modification specificity has been demonstrated before using the *C. elegans* HSN neuron [146]. In that context SDN-1 in the migrating neurons is modified by *hst-3.1* and *hst-6*. Conversely, *hst-2* and *hse-5* were found to modify other HSPGs involved in HSN migration.

Interestingly, our data indicated that *lin-44* and *egl-20* might interact with *sdn-1* via a specific combination of side chain modifications during axon outgrowth and then switch to other modified sites for axon termination. Our double mutant analysis suggests that during axon outgrowth *lin-44* is interacting with *sdn-1* through the sites that are modified by *hse-5.* While *egl-20* interacts with *sdn-1* at sites modified by *hse-5* and *hst-2.* Both modifying enzymes, *hst-2* and *hst-6* seem to be interacting with another yet unknown HSPG for this process since the loss of either with a Wnt ligand does not fully recapitulate the penetrance seen in *sdn-1*/Wnt double mutants. For axon termination *hse-5* seems to be important for the interaction between *sdn-1* and *lin-44*, while *egl-20* interacts with *sdn-1* via all three types of modifications. Again it is possible that these enzymes modify other proteins involved in both these processes and that other HSPGs and/ or ligands are modified. Further investigation could tease out the interactions and help us to further understand the mechanism behind axon outgrowth and termination.

Axon extension relies on proteins that are also involved in synaptogenesis

The incomplete effect on axon outgrowth in all of our mutant combinations, with the exception of *bar-1,* argues that multiple pathways function in a partially redundant fashion to regulate axon termination. For example, recent work has

indicated that the E3 ubiquitin ligase, RPM-1, and the synaptic scaffold protein, SYD-2, are also involved in axon termination [37, 147]. Similar to our results with *lin-44* and *egl-20,* the singular loss of *rpm-1* or *syd-2* did not result in under-extended axons, but double mutant animals did have shortened DNCs.

There have been a number of recent papers linking axon extension to synaptic development [142]. Multiple molecules function iteratively in these processes, *e.g. rpm-1, lin-44, etc.,* and, in *C. elegans,* disruption of the synapse of PLM neurons can stimulate axon outgrowth. Interestingly, at the *Drosophila* neuromuscular junction, syndecan adhesion can gate the developmental switch between synaptic stability and synaptic growth that occurs with organismal development. Going forward it will be important to determine if the axon outgrowth defects we observe are due to syndecan interacting with different ligands, or if they are entirely mediated through regulation of Wnt-dependent signaling.

Section 3.5 Materials and Methods

Strains and Genetics

N2 (var. Bristol) was used as the wild-type reference strain in all experiments. Strains were maintained at 18-22 ºC, using standard maintenance techniques as described [121]. Alleles used in this report include: *LGI, lin-44(n1792), lin-44(gk360814), lin-17(n671); LGII, mig-5(rh94); LGIV, egl-20(lq42)* (Erik Lundquist), *egl-20(gk453010), LGV, mom-2(or77); LGX bar-1(ga80), sdn-1(ok449), sdn-1(zh20), hse-5(tm472), hse-5(lq49), hst-2(ok595), hst-6(ok273).* The following transgenic lines were used: *lhIs47* [*Punc-25::mCherry*], *juIs76* [*Punc-25::gfp*], *muIs32* [*Pmec-7::gfp*], *juSi119* [*Psdn-1::SDN-1cDNA::GFP::sdn-1 3'UTR*] [30], wpSi12 [36], *lqIs80* [*Pscm::gfp*] (Erik Lundquist).

To generate hemizygous Mos-SCI we crossed N2 males to *sdn-1(zh20); juSi119* to generate *sdn-1/0; juSi119/+* males and crossed them with *sdn-1(zh20);juIs76*. The *juSi119* insertion rescues the male mating behavior absent from *zh20/0* males. We scored the resulting *sdn-1(zh20)*; *juSi119/juIs76* animals.

The *mom-2* RNAi experiments were conducted using a clone obtained from the Ahringer library (V-6A13;Overlapping CDS: F38E1.7) [63].

Plasmid Construction

sdn-1 cDNA was odtained by amplifying from a cDNA library, initially transcribed by random hexamers and Superscript III (Life Technologies). The primers used to amplify the cDNA were as follows: *sdn-1cDNAF1* 5' – caggtgattacaccaacaagac – 3' and *sdn-1cDNA R1* 5'- cagataagtgccatcagaaacc – 3'. The resulting PCR product was cloned into the pCR8/GW/Topo entry vector (Life

Technologies) and recombined into the *Punc-25* destination vector using LR recombinase (Life Technologies) using the manufacterer's protocol to generate pEVL449. The *sdn-1* cDNA was sequenced prior to recombination to ensure no errors were created by PCR.

Fluorescence microscopy

Axon termination in DD/VD motorneurons was visualized using the reporter strains, *juIs76* or *lhIs47* using an Olympus FV1000 confocal microscope. L4 larva and if necessary, as in the case with strains carrying *egl-20(lq42)lqIs80*, adult animals were assayed for proper axon termination. Animals where the DNC axons did not grow to the posterior edge of the cell bodies located on the VNC were considered under-extended. Animals in which the DNC axons grew past the cell bodies located on the VNC, were considered to be over-extended.

Statistics

A Fisher exact test was used to evaluate the statistical significance between various mutations and wild type. Significance values were calculated with GraphPad QuickCalcs (http://www.graphpad.com/quickcalcs/)

Section 3.6 Figures

Figure 3.1

A.

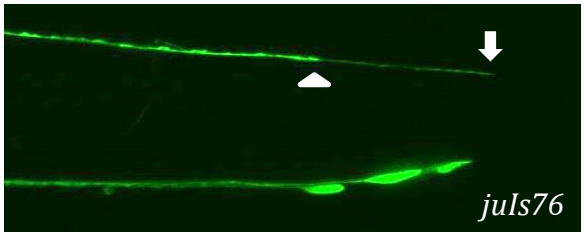

B.

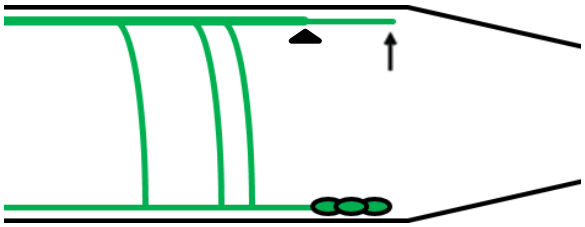

Figure 3.1 D-type motorneurons grow at stereotyped positions along the anterior-posterior axis (A) The most posterior D-type cells and their axons are visualized with juIs76 (Punc-25::GFP) in wild-type animals. The axons of DD6 and VD13 form a thick bundle that terminates just anterior to the position of the cell bodies in the VNC. The thin bundle consist of the VD13 axon that terminates at the posterior edge of the cell bodies in the VNC. (B) Schematic representation of D-type motor neurons. The VD12, DD6 and VD13 cell bodies (green ovals) in the ventral nerve cord. The arrow head marks the thick bundle termination and the arrow marks the thin bundle termination point.

Figure 3.2

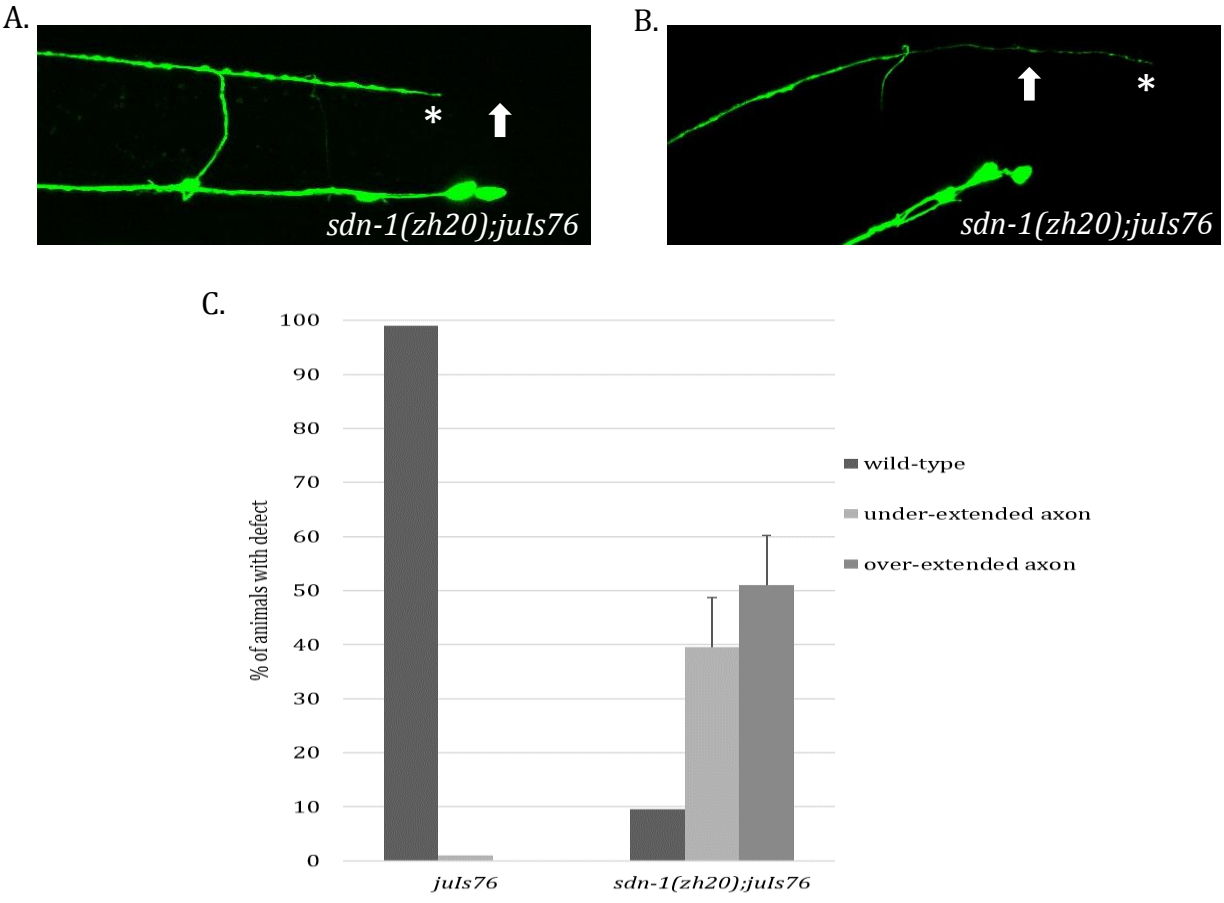
A.
sdn-1(zh20);juIs76
B.
sdn-1(zh20);juIs76
C.
% of animals with defect
100
90
80
70
60
50
40
30
20
10
0
juIs76
sdn-1(zh20);juIs76
wild-type
under-extended axon
over-extended axon

Figure 3.2 *sdn-1* is needed for D-type axon outgrowth and termination (A) Visualization of the under-extension phenotype seen in *sdn-1* LOF mutants. (B) Visualization of the over-extension phenotype seen in *sdn-1* LOF mutants. The arrow indicates the stereotypic termination point and the asterisk indicates the mutant termination point. The presence of both phenotypes indicates *sdn-1* functions in both axon outgrowth and axon termination. (C) Quantification of the phenotypes seen in *sdn-1* LOF mutants. Error bars represent the Standard Error of the Mean (SEM).

Figure 3.3

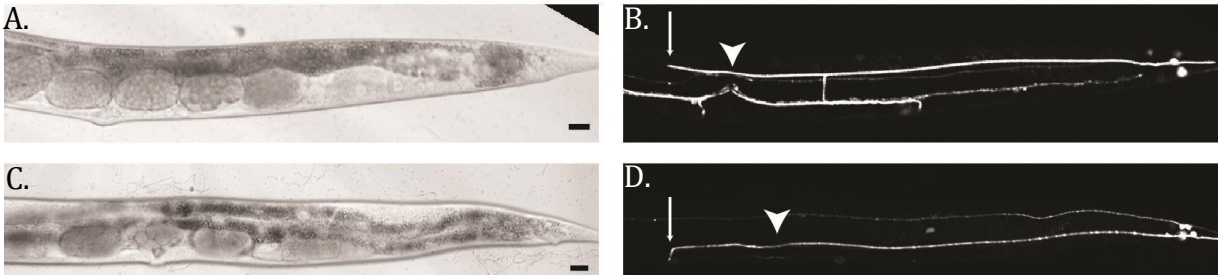

Figure 3.3 SDN-1 is a determinant of anterior-posterior axon guidance and termination in *C. elegans* (A, C) DIC and (B, D) fluorescent images of an L2 *sdn-1(zh20)* animal with *muIs32* (integrated GFP reporter expressed in the mechanosensory neurons ALM and PLM). (B) The PLM axons frequently terminated prematurely (not shown), but also failed to terminate growth. (D) The PLM axon would "hook" toward the ventral nerve cord. Arrow head indicates normal termination point and arrow indicates mutant termination point.

Figure 3.4

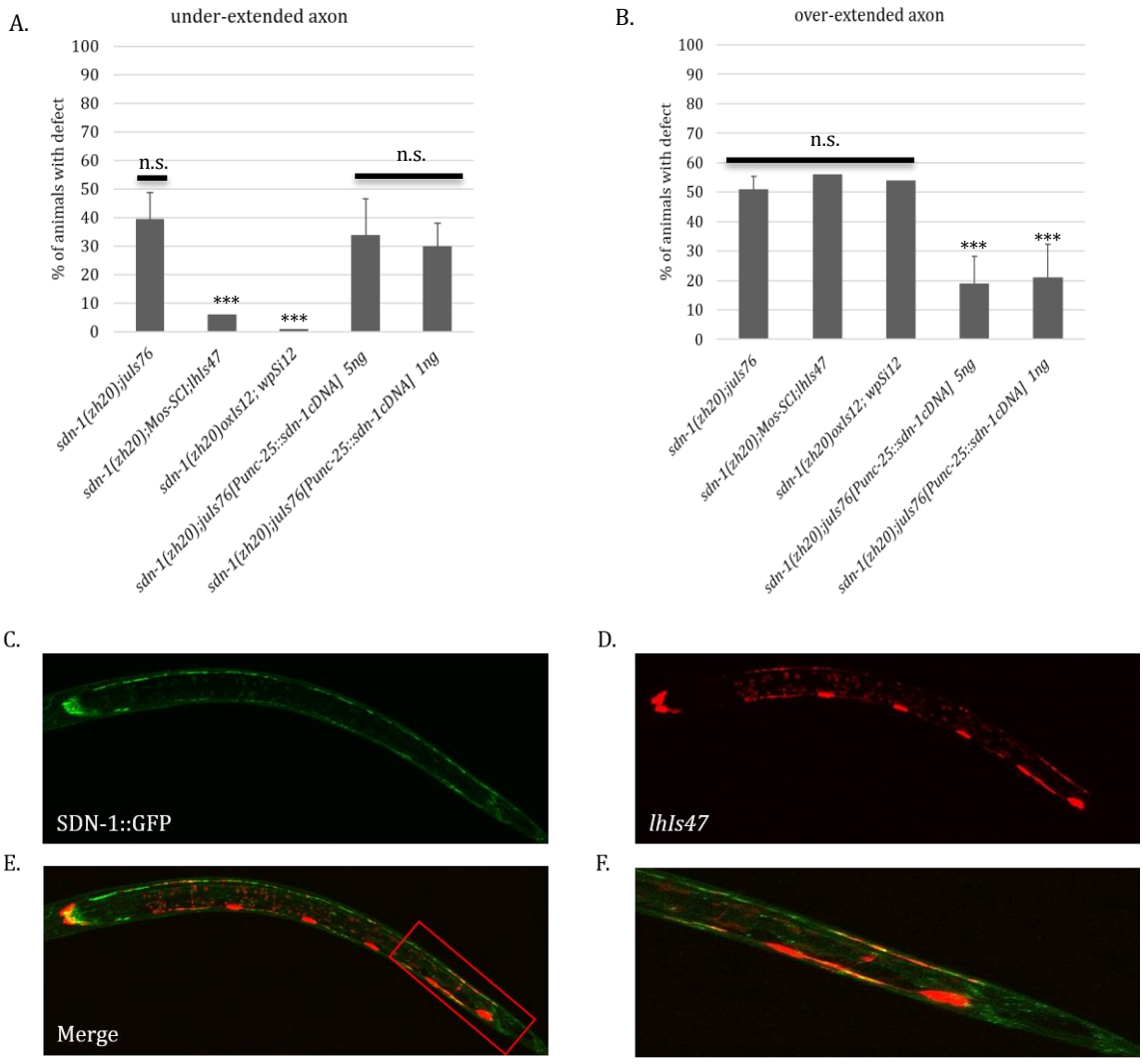
A.
under-extended axon
% of animals with defect
n.s.
n.s.
***
***
sdn-1(zh20);juIs76
sdn-1(zh20);Mos-SCI;lhIs47
sdn-1(zh20)oxIs12; wpSi12
sdn-1(zh20);juIs76[Punc-25::sdn-1cDNA] 5ng
sdn-1(zh20);juIs76[Punc-25::sdn-1cDNA] 1ng
B.
over-extended axon
% of animals with defect
n.s.
***
***
C.
SDN-1::GFP
D.
lhIs47
E.
Merge
F.

Figure 3.4 SDN-1 functions both cell autonomously and non-autonomously during axon outgrowth and termination (A) Quantification of the under-extension observed in SDN-1 Mos-SCI lines and *Punc-25::sdn-1cDNA* in *sdn-1(zh20)* mutants. (B) Quantification of the over-extension observed in SDN-1 Mos-SCI lines and *Punc-25::sdn-1cDNA* in *sdn-1(zh20)* mutants. N for *sdn-1(zh20);juIs76*= 200 animals, SDN-1::GFP Mos-SCI= 100 animals, *wpSi12* Mos-SCI= 100 animals, *Punc-25::sdn-1cDNA*= 60 animals and *Punc-25::sdn-1cDNA*= 100 animals. ***P=.0001. Statistical significance was calculated by using the Fisher's Exact Test. Error bars represent the Standard Error of the Mean (SEM). (C) Visualization of SDN-1::GFP in a L1 animal. The majority of expression is observed in the nervous system and hypodermal tissues. (D) Visualization of the D-type motorneurons using lhIs47 (*Punc-25*::mCherry). (E) Merge of the SDN-1::GFP and *lhIs47*. (D) Enlargement of the E panel. SDN-1:GFP can be seen co-expressed with *lhIs47* in the VNC, DNC and cell bodies.

Figure 3.5

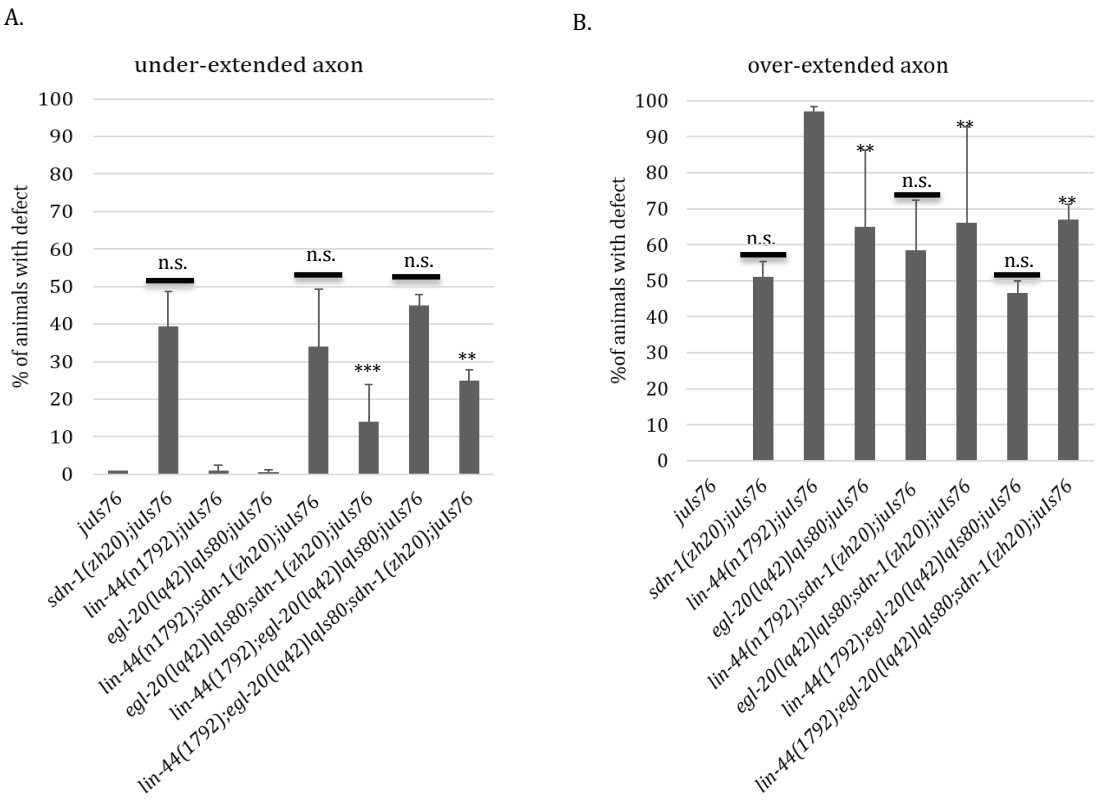
A.
under-extended axon
% of animals with defect
100
90
80
70
60
50
40
30
20
10
0
n.s.
n.s.
n.s.
***
**
juIs76
sdn-1(zh20);juIs76
lin-44(n1792);juIs76
egl-20(lq42)lqIs80;juIs76
lin-44(n1792);sdn-1(zh20);juIs76
egl-20(lq42)lqIs80;sdn-1(zh20);juIs76
lin-44(1792);egl-20(lq42)lqIs80;juIs76
lin-44(1792);egl-20(lq42)lqIs80;sdn-1(zh20);juIs76
B.
over-extended axon
%of animals with defect
100
90
80
70
60
50
40
30
20
10
0
n.s.
**
n.s.
**
n.s.
**
juIs76
sdn-1(zh20);juIs76
lin-44(n1792);juIs76
egl-20(lq42)lqIs80;juIs76
lin-44(n1792);sdn-1(zh20);juIs76
egl-20(lq42)lqIs80;sdn-1(zh20);juIs76
lin-44(1792);egl-20(lq42)lqIs80;juIs76
lin-44(1792);egl-20(lq42)lqIs80;sdn-1(zh20);juIs76

Figure 3.5 *sdn-1* functions with Wnt ligands for axon outgrowth and termination (A) Quantification of the under-extension phenotype seen in *sdn-1* as compared to Wnt single and double mutant animals. The under-extension seen in *sdn-1* is not significantly different than *lin-44(n1792);sdn-1(zh20)* and *lin-44(n1792);egl-20(lq42)lqIs80;lhIs47*. (B) Quantification of the over-extension phenotype seen in *sdn-1* as compared to Wnt single and double mutant animals. The over-extension seen in *sdn-1* is not significantly different than *lin-44(n1792);sdn-1(zh20)* and *lin-44(n1792);egl-20(lq42)lqIs80;lhIs47*. ***P= .0001, **P= .002. N= 200 animals. Statistical significance was calculated by using the Fisher's Exact Test. Error bars represent the Standard Error of the Mean (SEM). L4 animals were analyzed except when *lqIs80* was present then adult animals were scored.

Figure 3.6

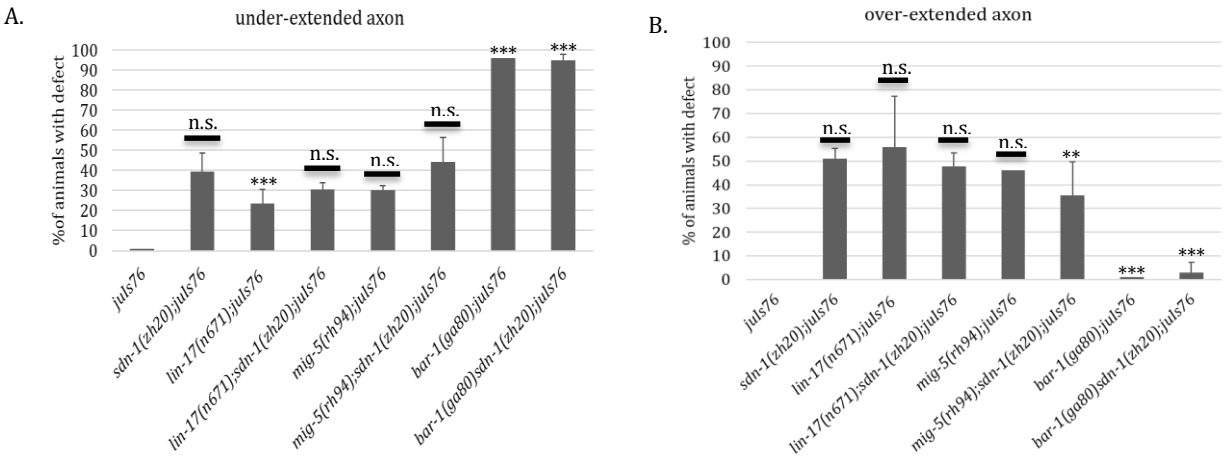
A.
under-extended axon
%of animals with defect
100
90
80
70
60
50
40
30
20
10
0
n.s.
***
n.s.
n.s.
n.s.
***
***
juIs76
sdn-1(zh20);juIs76
lin-17(n671);juIs76
lin-17(n671);sdn-1(zh20);juIs76
mig-5(rh94);juIs76
mig-5(rh94);sdn-1(zh20);juIs76
bar-1(ga80);juIs76
bar-1(ga80)sdn-1(zh20);juIs76
B.
over-extended axon
% of animals with defect
100
90
80
70
60
50
40
30
20
10
0
n.s.
n.s.
n.s.
n.s.
**
***
***
juIs76
sdn-1(zh20);juIs76
lin-17(n671);juIs76
lin-17(n671);sdn-1(zh20);juIs76
mig-5(rh94);juIs76
mig-5(rh94);sdn-1(zh20);juIs76
bar-1(ga80);juIs76
bar-1(ga80)sdn-1(zh20);juIs76

Figure 3.6 *sdn-1* functions with canonical Wnt signaling effectors (A) Quantification of the under-extension phenotype seen in *sdn-1* as compared to Wnt effector single and double mutant animals. The under-extension seen in *sdn-1* is not significantly different than *lin-17(n671);sdn-1(zh20)*, *mig-5(rh94)* and *mig-5(rh94);sdn-1(zh20)*. ***P<.0009 N>100 (B) Quantification of the over-extension phenotype seen in *sdn-1* as compared to Wnt effector single and double mutant animals. The over-extension seen in *sdn-1* is not significantly different than *lin-17(n671)*, *lin-17(n671);sdn-1(zh20)*, and *mig-5(rh94)*. ***P=.0001 **P= .004 N>100. Statistical significance was calculated by using the Fisher's Exact Test. Error bars represent the Standard Error of the Mean (SEM).

Figure 3.7

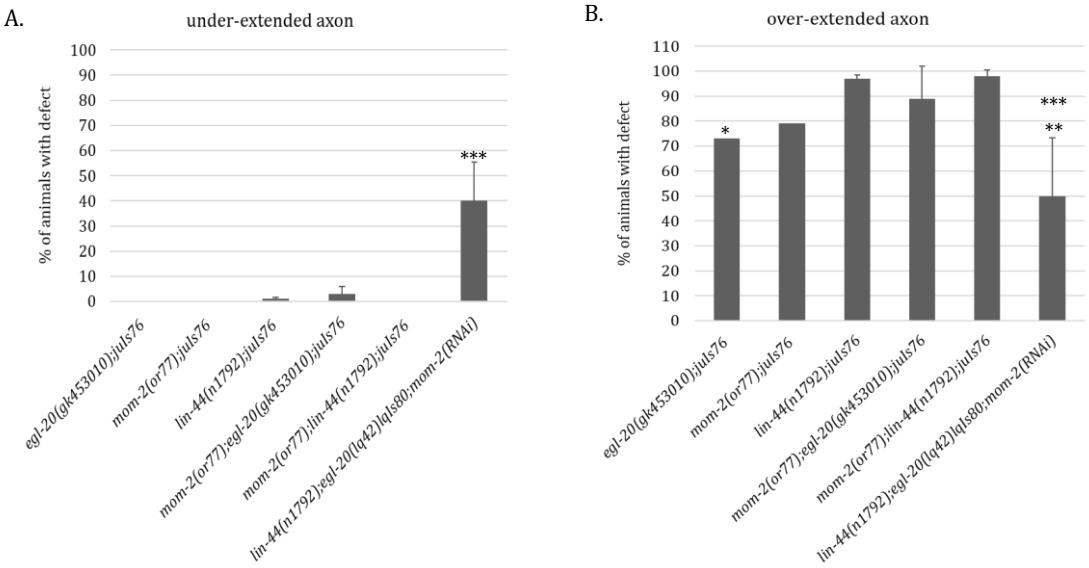
A.
under-extended axon
% of animals with defect
100
90
80
70
60
50
40
30
20
10
0
***
egl-20(gk453010);juIs76
mom-2(or77);juIs76
lin-44(n1792);juIs76
mom-2(or77);egl-20(gk453010);juIs76
mom-2(or77);lin-44(n1792);juIs76
lin-44(n1792);egl-20(lq42)lqIs80;mom-2(RNAi)
B.
over-extended axon
% of animals with defect
110
100
90
80
70
60
50
40
30
20
10
0
*
***
**
egl-20(gk453010);juIs76
mom-2(or77);juIs76
lin-44(n1792);juIs76
mom-2(or77);egl-20(gk453010);juIs76
mom-2(or77);lin-44(n1792);juIs76
lin-44(n1792);egl-20(lq42)lqIs80;mom-2(RNAi)

Figure 3.7 *mom-2* does not act redundantly with *lin-44* or *egl-20* during D-type motorneuron axon outgrowth and termination (A) Quantification of the under-extension phenotype seen in Wnt ligand single and double genetic mutant animals and *lin-44;egl-20* animals grown on bacteria expressing *mom-2* dsRNA. We found no evidence of under-extension in *mom-2(or77)*. Double mutants of *mom-2(or77)* with *lin-44(n1792)* (0%) and *egl-20(gk453010)* (3%) did not result in under-extension defects. The under-extension observed in the *lin-44;egl-20;mom-2(RNAi)* (40%) was not significantly different than *lin-44;egl-20* mutants (45%). (B) Quantification of the over-extension phenotype seen in Wnt ligand single and double genetic mutant animals and *lin-44;egl-20* animals grown on bacteria expressing *mom-2* dsRNA. LOF of *mom-2* via RNAi caused a significant decrease in over-extension defects seen in *lin-44(n1792)* or *egl-20(gk453010)*. However, the loss of *mom-2* in a *lin-44;egl-20* background (50%) was not significantly different from *lin-44;egl-20* (46.5%). ***P=.0002, **P=.004, *P=.02 N>60. Statistical significance was calculated by using the Fisher's Exact Test. Error bars represent the Standard Error of the Mean (SEM).

Figure 3.8

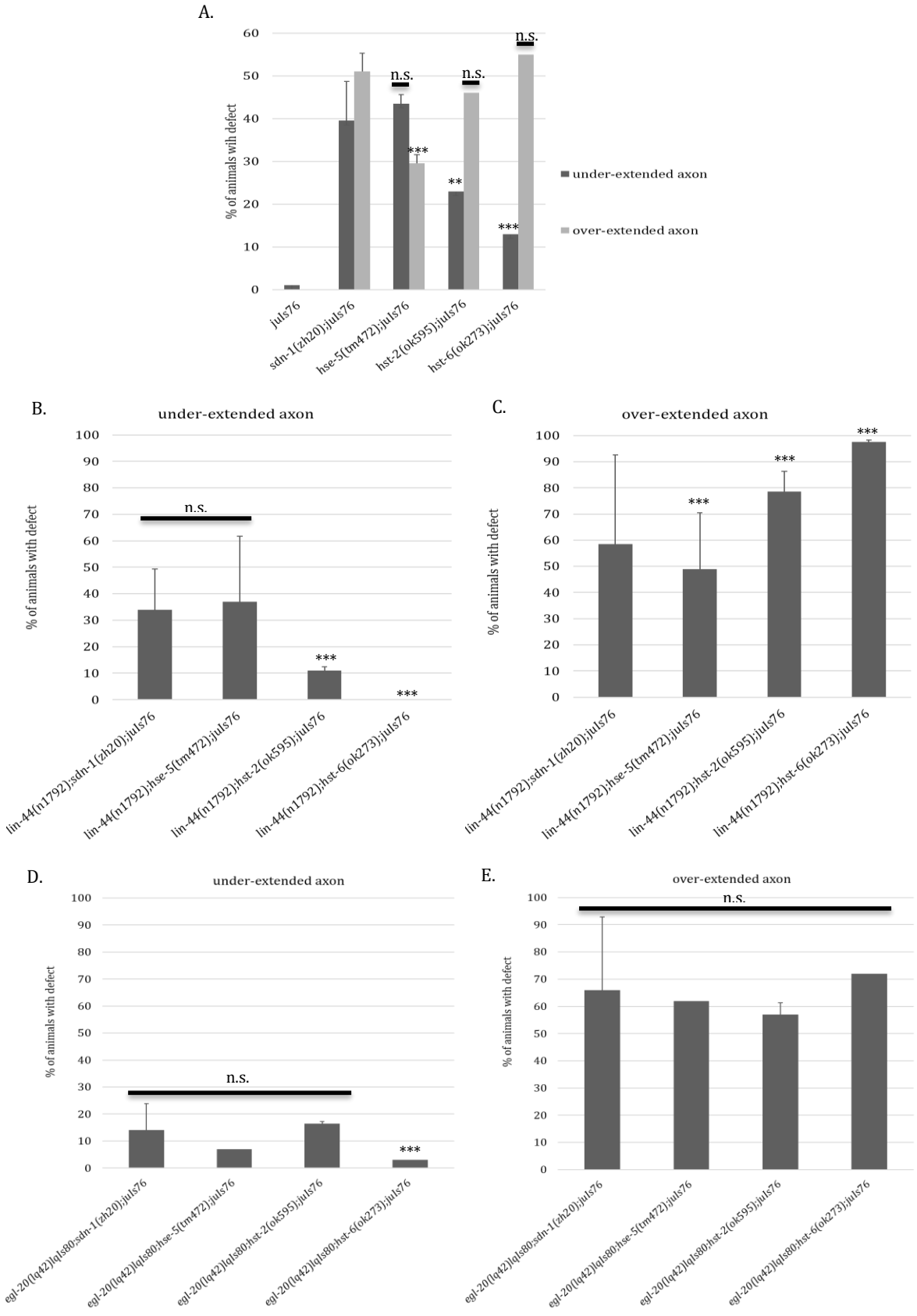
A.
% of animals with defect
under-extended axon
over-extended axon
n.s.
***
**
juIs76
sdn-1(zh20);juIs76
hse-5(tm472);juIs76
hst-2(ok595);juIs76
hst-6(ok273);juIs76
B.
under-extended axon
C.
over-extended axon
lin-44(n1792);sdn-1(zh20);juIs76
lin-44(n1792);hse-5(tm472);juIs76
lin-44(n1792);hst-2(ok595);juIs76
lin-44(n1792);hst-6(ok273);juIs76
D.
under-extended axon
E.
over-extended axon
egl-20(lq42)lqIs80;sdn-1(zh20);juIs76
egl-20(lq42)lqIs80;hse-5(tm472);juIs76
egl-20(lq42)lqIs80;hst-2(ok595);juIs76
egl-20(lq42)lqIs80;hst-6(ok273);juIs76

Figure 3.8 *sdn-1* heparan sulfate side chain modifications are important for Wnt interactions (A) Quantification of under- and over-extension defects observed in *hse-5(tm472)*, *hst-2(ok595)* and *hst-6(ok273)* compared to *sdn-1(zh20)***.** Loss of either *hst-2* (23%) or *hst-6* (13%) does not fully recapitulate the under-extension defects seen in *sdn-1* (39.5%)**.** While *hse-5* (43.5%), under-extension is not significantly different than *sdn-1* (39.5%), the over-extension is significantly decreased (29% vs. 51%). (B-C) Quantification of under- and over-extension defects observed in *lin-44(n1792)*, *hse-5(tm472)*, *hst-2(ok595)* and *hst-6(ok273)* double mutants compared to *lin-44(n1792);sdn-1(zh20)***.** (D-E) Quantification of under- and over-extension defects observed in *egl-20(lq42)*, *hse-5(tm472)*, *hst-2(ok595)* and *hst-6(ok273)* double mutants compared to *egl-20(lq42);sdn-1(zh20)***.** N>100. ***P= .0001, **P<.03. Statistical significance was calculated by using the Fisher's Exact Test. Error bars represent the Standard Error of the Mean (SEM). Experiments and analysis were conducted by Samantha Hartin and Riley Roberts.

Figure 3.9

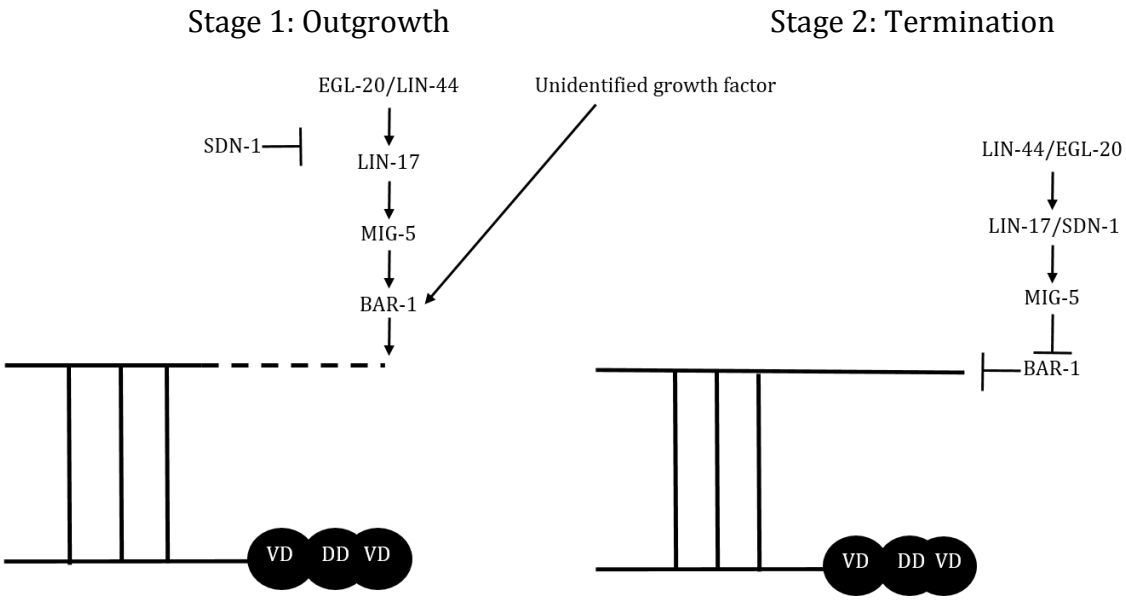
Stage 1: Outgrowth
Stage 2: Termination
EGL-20/LIN-44
Unidentified growth factor
SDN-1
LIN-17
MIG-5
BAR-1
VD
DD
VD
LIN-44/EGL-20
LIN-17/SDN-1
MIG-5
BAR-1
VD
DD
VD

Figure 3.9 Genetic model for D-type axon outgrowth and termination (Stage 1: Outgrowth) SDN-1 is most likely inhibiting Wnt signaling and the downstream effectors to allow for proper axon outgrowth. (Stage 2: Termination) Since we were able to partially rescue the over-growth phenotype by specifically expressing SDN-1 in the D-type neurons. This suggests that SDN-1 can in the D-type motorneurons to activate the Wnt signaling pathway and allow for proper axon termination. This is consistent with our genetic data that the loss of *sdn-1* and *lin-17* are both associated with outgrowth errors.

Chapter IV
Concluding remarks and future directions

Section 4.1 Concluding remarks

The findings in Chapter II reveal roles for PTP-3 and SDN-1 during *C. elegans* embryogenesis and larval development. Here using double mutant and 4D time lapse analysis we found that PTP-3 and SDN-1 work in parallel pathways to ensure proper epidermal development. Using the SynLet phenotype seen in the *ptp-3;sdn-1* double mutants, we conducted an RNAi screen for other ECM molecules that could interact with either gene during development. Our sensitized backgrounds allowed for identification of molecules that may have been missed in traditional screens due to low phenotypic penetrance. It is important to note that we may have missed certain genes during our screen due to the nature of RNAi (Off target effects, reduced induction or inherent resistance). Regardless, identification of genes previously shown to be involved with either *ptp-3* or *sdn-1* suggests that our method is a valid way to identify genetic interactions using genes of interest.

One such gene *lin-44*, a Wnt ligand, was identified as been SynLet with *sdn-1* but not *ptp-3* suggesting that it may function in a linear pathway with *ptp-3* that functions in parallel to *sdn-1*. Again using double mutants and 4D time lapse analysis we found that complete LOF mutations in *lin-44* and *sdn-1* cause the majority of animals to arrest at the embryo stage. This arrest is due to the improper migration of endodermal precursor cells Ea and Ep at the 24-cell stage of development. Normally LIN-44 signals through the Frizzled receptor LIN-17. However, we believe that during this process LIN-44 does not function through its canonical Frizzled receptor, LIN-17, due to the level of embryonic lethality observed in *lin-17;sdn-1* double mutants. Double mutant analysis of *ptp-3* and *lin-44* revealed no significant increase in

embryonic lethality, although the level of larval lethality increased slightly when compared to each single mutant. This suggests that *lin-44* and *ptp-3* may be functioning in the same genetic pathway during embryonic development.

Our results are consistent with the idea that *ptp-3* contributes to *lin-44*-dependent embryogenesis. Furthermore, it is likely that at least one of the potential reasons that *ptp-3; sdn-1* double mutants exhibit SynLet is because of a disruption in a *lin-44 / ptp-3* signaling pathway during gastrulation.

Chapter III identifies later functions for SDN-1, LIN-44 and EGL-20 during motorneuron axon outgrowth and termination. Additionally, our results show that another yet unidentified signaling molecule functions during both these processes. Our studies complement previous genetic data suggesting that LIN-44 and EGL-20 work together for proper axon termination of the most posterior DD/VD motorneurons in the *C. elegans* tail. However, our complete LOF double mutant analysis also suggests that both genes function in DD/VD axon outgrowth, but the importance of each molecule differs during the two processes. Here, we found that SDN-1 functions in both processes. During the first process, SDN-1 is required non-autonomously to regulate Wnt signaling either by controlling the diffusion/distribution of the Wnt ligands or by disrupting the Wnt-Frizzled interaction (Figure 4.1). For proper axon termination, SDN-1 acts cell autonomously to inhibit Wnt signaling, perhaps by binding to MIG-5 to disrupt its ability to inhibit the β-catenin destruction complex (Figure 4.1). Further genetic analysis of the downstream Wnt effectors indicate that SDN-1 functions at the level of the Frizzled receptor LIN-17 and possibly with Dishevelled/MIG-5 during both processes.

Interestingly, loss of *bar-1* causes the axons to under-extend in 95% of animals suggesting that BAR-1 activity is negatively regulated for axon extension through SDN-1 inhibition of proper Wnt signaling.

The HS side chains of SDN-1 are important for ligand interactions. By analyzing the enzymes that modify the side chains (HSE-5, HST-2 and HST-6) we found that they have functions in both processes. However, none of them were able to recapitulate the phenotypic penetrance seen in *sdn-1* single or *sdn*-1*;Wnt* double mutants. These data suggest that there are other modifying enzymes that function during these processes, and possibly other proteoglycans as well.

Overall, our genetic analyses indicate that SDN-1 is needed for both DD/VD motorneuron axon extension and termination because LOF *sdn-1* mutants display both under and over-extension defects. We propose a two stage model where EGL-20 and LIN-44 signal through LIN-17, SDN-1, MIG-5 and BAR-1 to regulate axon extension. Here SDN-1 acts as a negative regulator of β-catenin dependent Wnt signaling. Additionally, our findings regarding the extent of over-extension phenotypes lead us to hypothesize that EGL-20 plays a larger role with SDN-1 than LIN-44 during this initial stage. When the axon reaches the proper termination point LIN-44 and EGL-20 again use LIN-17, SDN-1 and MIG-5 to signal for axon termination. During this second stage we believe that LIN-44 is acting as the primary molecule used for termination in a parallel pathway to EGL-20 and SDN-1, and these two pathways converge on the same molecule at some point. Since none of the complete LOF mutations recapitulate the phenotypes seen in the triple mutant we believe there

is another molecule involved in axon extension and termination. Further studies will be needed to confirm this hypothesis.

In conclusion, the results presented in this dissertation describe how known cell adhesion molecules function initially in parallel pathways during gastrulation and later function in the same pathway during neural development. Both the identification of the role of LIN-44 during gastrulation alongside PTP-3 and SDN-1 and the later characterization of the SDN-1/Wnt interaction add to the current knowledge of how these molecules are reused during development. We also identified an effective way to search for genes of interest using a sensitized reverse genetics approach.

Section 4.2 Future Directions

The findings presented in this dissertation provide new insights into the reuse of cell adhesion molecules during development. However, some questions remain unanswered. Going forward, addressing the following questions will further our knowledge of how SDN-1 and the Wnt pathways intersect during embryogenesis and axon guidance.

Question 1: Where is SDN-1 functioning during axon outgrowth and termination?

In chapter III we demonstrated that LOF mutations in *sdn-1* cause both under and over-extension of the DD6 and/or VD13 axons in the dorsal nerve cord, suggesting SDN-1 is involved in both axon extension and termination. Our genetic analysis of SDN-1 and the Wnt pathway suggest that SDN-1 works in combination with both LIN-44 and EGL-20 during both processes. However, we do not know where SDN-1 is functioning in these processes. Previous studies of Wnt receptors showed that they can work both cell autonomously and non-autonomously to modulate Wnt signaling. We hypothesize that SDN-1 has both a cell autonomous and non-autonomous role and switches between these roles during axon outgrowth and axon termination in response to the different Wnt signals.

SDN-1 is expressed in multiple tissues throughout *C. elegans* development including the nervous system, hypodermis and pharynx [15, 99]. Expression of full length SDN-1 in either the nervous system or hypodermis can rescue different phenotypes seen in LOF *sdn-1* mutants [15]

We found that under-extension of the DD/VD axons can be rescued by reintroducing a single copy of the full length SDN-1 gene back into *sdn-1* mutants. However, the over-extension phenotype is not fully rescued. This partial phenotypic rescue has also been reported by others [30, 36]. This partial result suggests that there are long distance regulatory elements and/or genomic positional requirements that have yet to be identified, which are necessary for full rescue of the *sdn-1* phenotypes.

Since we did not obtain full rescue with two separate SDN-1 Mos-SCI lines, we made a SDN-1 cDNA construct that is expressed in the VD/DD motorneurons by the *unc-25* promoter. We analyzed two separate injection concentrations and found that neither fully rescued either phenotype but we were able to significantly decrease penetrance of the over-extension defects seen in *sdn-1* LOF mutants. Next, we made SDN-1 cDNA constructs driven by the *myo-3* promoter, which drives expression in the muscles. With this construct we were able to significantly decrease the penetrance of over-extended axons however the penetrance of under-extended axons increased significantly.

We will need to determine whether the defects can be rescued by the SDN-1 cDNA alone and if it can rescue our phenotypes under its endogenous promoter. We will also need to express our SDN-1 cDNA from the hypodermis to determine if SDN-1 functions there during either process. However, similar constructs have not been able to fully rescue all *sdn-1* phenotypes including axon guidance [15, 36]. Mosaic analysis may also be employed to determine where SDN-1 is functioning during axon outgrowth and termination.

Question 2: Does SDN-1 physically interact with components of the Wnt pathway?

According to the genetic data presented in this dissertation, SDN-1 acts at the level of LIN-17/Frizzled and/or MIG-5/Dishevelled during each stage. However, it is unknown whether these molecules are physically interacting during signaling. Interactions between HSPGs and Frizzled receptors are reported to be important in the positive and negative regulation of Wnt signaling [30-33, 35]. We have imaged and analyzed animals with SDN-1::GFP and LIN-17::RFP and found that both are broadly localized in the animal. SDN-1::GFP is prominent in the dorsal nerve cord and LIN-17::RFP is also present in the DNC. Closer analysis show SDN-1::GFP and LIN-17::RFP signals at the axon termination point (Figure 4.2). Our initial FRET (Fluorescence resonance energy transfer) analysis of SDN-1 and LIN-17 suggest that they are closely situated in the both the dorsal and ventral nerve cords but, their association is more prevalent in the dorsal nerve cord. These data suggest that they may physically interact in those axons. To determine whether SDN-1 and LIN-17 are physically interacting we could conduct CO-IP assays in wild-type and mutant strains.

SDN-1 may also be physically interacting with MIG-5/Dishevelled via its PDZ domain. To determine if this is important for proper Wnt signaling we could repeat the above assays substituting LIN-17 reagents for MIG-5 reagents.

Section 4.3 Figures

Figure 4.1

A.

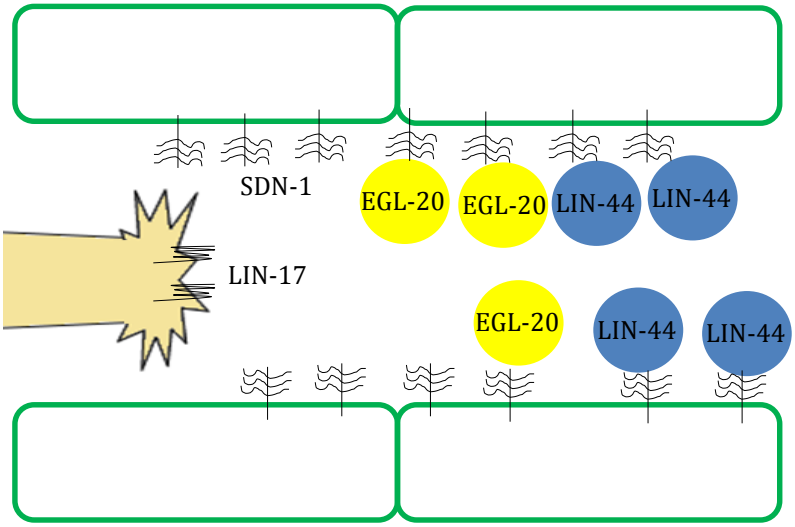

B.

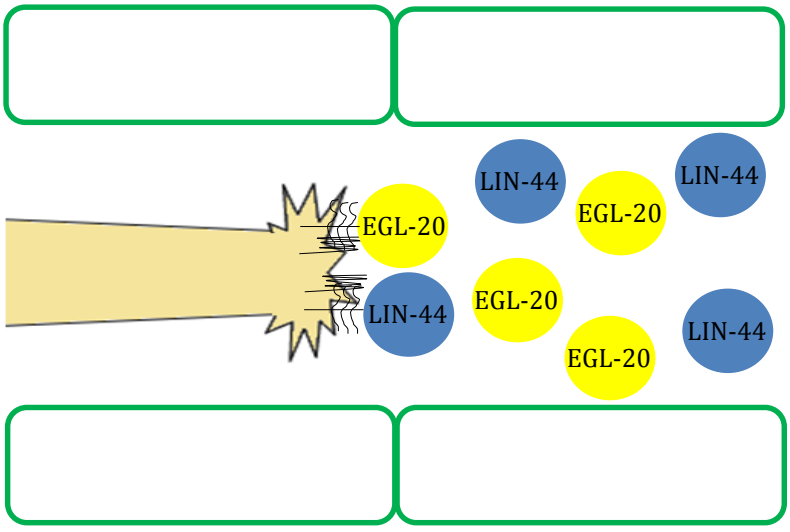

Figure 4.1 Potential molecular model for the two step growth of the D-type motorneurons Our results suggest that these functions are likely mediated by different cells expressing SDN-1. (A) When we replaced SDN-1 function broadly using Mos-SCI constructs we found that we could only rescue the under-extension of axons, but could partially rescue the under-extension when we decreased the levels of SDN-1 by making the integrated transgene heterozygous. These results indicate that SDN-1 is acting outside the D-type motorneurons to inhibit Wnt signaling. Possibly by restricting the distribution of the ligands. (B) We were able to partially rescue the over-growth phenotype by specifically expressing SDN-1 in the D-type neurons. This suggests that SDN-1 can function cell-autonomously in the D-type neurons to restrict outgrowth. It is possible that SDN-1 is acting to promote Wnt signaling, via LIN-17, at the termination point of the D-type neurons, to inhibit further growth.

Figure 4.2

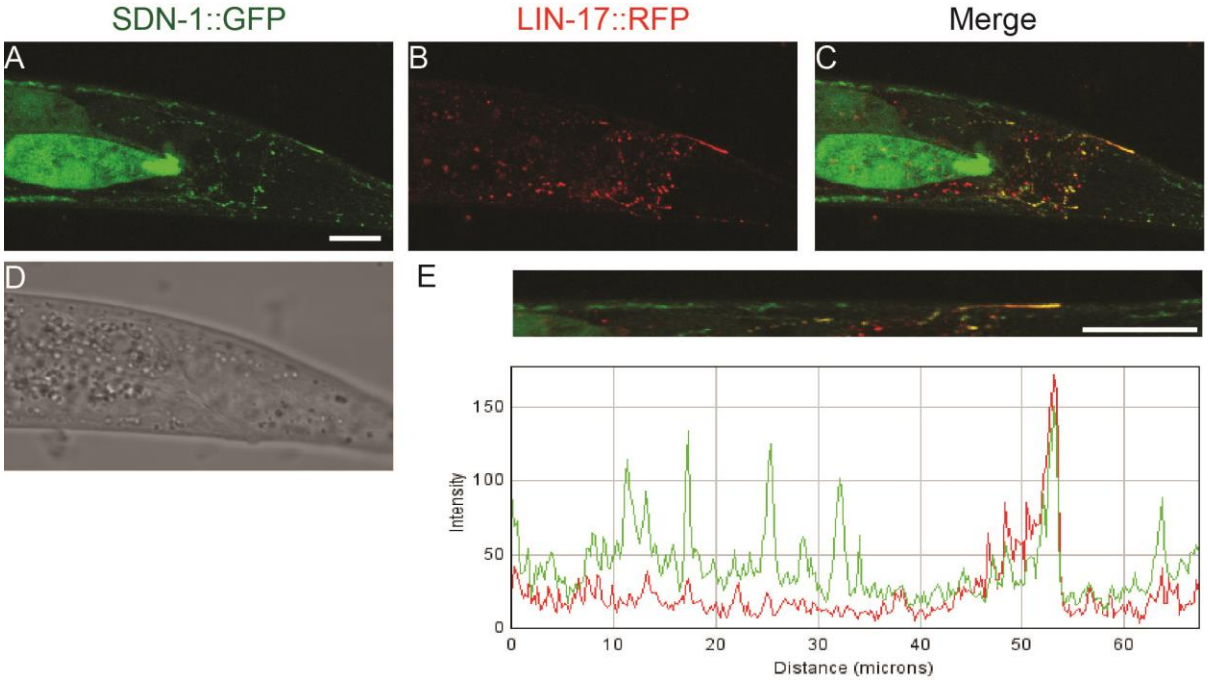
SDN-1::GFP
LIN-17::RFP
Merge
A
B
C
D
E
150
100
50
0
Intensity
0
10
20
30
40
50
60
Distance (microns)

Figure 4.2 SDN-1 and LIN-17 are present at the approximate termination point of the D-type motorneurons in the dorsal nerve cord (A) SDN-1::GFP is broadly localized in the animal, but is prominent in the dorsal nerve cord (DNC) and there is a concentration of SDN-1::GFP (arrow) just dorsal to the intestinal-rectal junction, the position where the GABAergic axons terminate in wild type animals. (B) LIN-17::RFP is also present throughout the animal, including in the DNC. (C) DIC image of animal. (D, E) An enlarged region of the DNC at the termination point. (F) A merge of the SDN-1::GFP and LIN-17::RFP signals demonstrating they are coincident at the termination point. (G) A line scan along the DNC region depicted demonstrates that the SDN-1::GFP intensity is higher near the termination point. LIN-17::RFP, while not enriched is present in punctate form along the DNC, but is not enriched after the termination point. Scale bar in A is equivalent to 10 μm, scale bar in D is equivalent to 1 μm. Experiment and image analysis done by Dr. Brian Ackley.

References

1. Skach, W.R., *The expanding role of the ER translocon in membrane protein folding.* The Journal of cell biology, 2007. **179**(7): p. 1333-1335.
2. Pickart, M.A., et al., *Genome-wide reverse genetics framework to identify novel functions of the vertebrate secretome.* PLoS One, 2006. **1**(1): p. e104.
3. Klee, E.W., et al., *Identifying secretomes in people, pufferfish and pigs.* Nucleic acids research, 2004. **32**(4): p. 1414-1421.
4. Suh, J. and H. Hutter, *A survey of putative secreted and transmembrane proteins encoded in the C. elegans genome.* BMC genomics, 2012. **13**(1): p. 333.
5. Krieg, T. and E. Carwile LeRoy, *Diseases of the extracellular matrix.* Journal of Molecular Medicine, 1998. **76**(3): p. 224-225.
6. Lu, P., et al., *Extracellular matrix degradation and remodeling in development and disease.* Cold Spring Harbor perspectives in biology, 2011. **3**(12): p. a005058.
7. Johnson, K.G., et al., *The HSPGs Syndecan and Dallylike bind the receptor phosphatase LAR and exert distinct effects on synaptic development.* Neuron, 2006. **49**(4): p. 517-531.
8. Kaufmann, N., et al., *Drosophila liprin-α and the receptor phosphatase Dlar control synapse morphogenesis.* Neuron, 2002. **34**(1): p. 27-38.
9. Sundararajan, L., et al., *The fat-like cadherin CDH-4 acts cell-non-autonomously in anterior–posterior neuroblast migration.* Developmental biology, 2014. **392**(2): p. 141-152.
10. Johnson, K.G. and D. Van Vactor, *Receptor protein tyrosine phosphatases in nervous system development.* Physiological reviews, 2003. **83**(1): p. 1-24.
11. Ackley, B.D., et al., *The two isoforms of the Caenorhabditis elegans leukocyte-common antigen related receptor tyrosine phosphatase PTP-3 function independently in axon guidance and synapse formation.* The Journal of neuroscience, 2005. **25**(33): p. 7517-7528.
12. Harrington, R.J., et al., *The C. elegans LAR-like receptor tyrosine phosphatase PTP-3 and the VAB-1 Eph receptor tyrosine kinase have partly redundant functions in morphogenesis.* Development, 2002. **129**(9): p. 2141-2153.
13. Sundararajan, L. and E.A. Lundquist, *Transmembrane Proteins UNC-40/DCC, PTP-3/LAR, and MIG-21 Control Anterior–Posterior Neuroblast Migration with Left–Right Functional Asymmetry in Caenorhabditis elegans.* Genetics, 2012. **192**(4): p. 1373-1388.
14. Chin-Sang, I.D., et al., *The divergent C. elegans ephrin EFN-4 functions inembryonic morphogenesis in a pathway independent of the VAB-1 Eph receptor.* Development, 2002. **129**(23): p. 5499-5510.
15. Rhiner, C., et al., *Syndecan regulates cell migration and axon guidance in C. elegans.* Development, 2005. **132**(20): p. 4621-4633.
16. Hudson, M.L., et al., *C. elegans Kallmann syndrome protein KAL-1 interacts with syndecan and glypican to regulate neuronal cell migrations.* Developmental biology, 2006. **294**(2): p. 352-365.

17. Díaz-Balzac, C.A., et al., *Complex Cooperative Functions of Heparan Sulfate Proteoglycans Shape Nervous System Development in Caenorhabditis elegans.* G3: Genes| Genomes| Genetics, 2014. **4**(10): p. 1859-1870.
18. Silhankova, M. and H.C. Korswagen, *Migration of neuronal cells along the anterior–posterior body axis of C. elegans: Wnts are in control.* Current opinion in genetics & development, 2007. **17**(4): p. 320-325.
19. Prasad, B.C. and S.G. Clark, *Wnt signaling establishes anteroposterior neuronal polarity and requires retromer in C. elegans.* Development, 2006. **133**(9): p. 1757-1766.
20. Lu, C.S. and D. Van Vactor, *Synapse specificity: Wnts keep motor axons on target.* Current Biology, 2007. **17**(20): p. R895-R898.
21. Zinovyeva, A.Y., et al., *Complex network of Wnt signaling regulates neuronal migrations during Caenorhabditis elegans development.* Genetics, 2008. **179**(3): p. 1357-1371.
22. Sánchez‐Camacho, C. and P. Bovolenta, *Emerging mechanisms in morphogen‐mediated axon guidance.* Bioessays, 2009. **31**(10): p. 1013-1025.
23. Logan, C.Y. and R. Nusse, *The Wnt signaling pathway in development and disease.* Annu. Rev. Cell Dev. Biol., 2004. **20**: p. 781-810.
24. Chien, A.J., W.H. Conrad, and R.T. Moon, *A Wnt survival guide: from flies to human disease.* Journal of Investigative Dermatology, 2009. **129**(7): p. 1614-1627.
25. White, J.G., et al., *The structure of the nervous system of the nematode Caenorhabditis elegans.* Philosophical Transactions of the Royal Society of London. B, Biological Sciences, 1986. **314**(1165): p. 1-340.
26. Wightman, B., R. Baran, and G. Garriga, *Genes that guide growth cones along the C. elegans ventral nerve cord.* Development, 1997. **124**(13): p. 2571-2580.
27. Durbin, R.M., *Studies on the development and organisation of the nervous system of Caenorhabditis elegans*. 1987, University of Cambridge UK.
28. Garriga, G., C. Desai, and H.R. Horvitz, *Cell interactions control the direction of outgrowth, branching and fasciculation of the HSN axons of Caenorhabditis elegans.* Development, 1993. **117**(3): p. 1071-1087.
29. Sulston, J.E., et al., *The embryonic cell lineage of the nematode Caenorhabditis elegans.* Developmental biology, 1983. **100**(1): p. 64-119.
30. Dejima, K., et al., *Syndecan defines precise spindle orientation by modulating Wnt signaling in C. elegans.* Development, 2014. **141**(22): p. 4354-65.
31. Schwabiuk, M., L. Coudiere, and D.C. Merz, *SDN-1/syndecan regulates growth factor signaling in distal tip cell migrations in C. elegans.* Developmental biology, 2009. **334**(1): p. 235-242.
32. Ohkawara, B., A. Glinka, and C. Niehrs, *Rspo3 binds syndecan 4 and induces Wnt/PCP signaling via clathrin-mediated endocytosis to promote morphogenesis.* Developmental cell, 2011. **20**(3): p. 303-314.
33. Lin, X., *Functions of heparan sulfate proteoglycans in cell signaling during development.* Development, 2004. **131**(24): p. 6009-6021.

34. Bishop, J.R., M. Schuksz, and J.D. Esko, *Heparan sulphate proteoglycans fine-tune mammalian physiology.* Nature, 2007. **446**(7139): p. 1030-1037.
35. Gagliardi, M., E. Piddini, and J.P. Vincent, *Endocytosis: a positive or a negative influence on Wnt signalling?* Traffic, 2008. **9**(1): p. 1-9.
36. Edwards, T.J. and M. Hammarlund, *Syndecan Promotes Axon Regeneration by Stabilizing Growth Cone Migration.* Cell reports, 2014. **8**(1): p. 272-283.
37. Opperman, K.J. and B. Grill, *RPM-1 is localized to distinct subcellular compartments and regulates axon length in GABAergic motor neurons.* Neural development, 2014. **9**(1): p. 10.
38. Gysi, S., et al., *A network of HSPG core proteins and HS modifying enzymes regulates netrin-dependent guidance of D-type motor neurons in Caenorhabditis elegans.* PloS one, 2013. **8**(9): p. e74908.
39. Huang, X., et al., *MAX-1, a novel PH/MyTH4/FERM domain cytoplasmic protein implicated in netrin-mediated axon repulsion.* Neuron, 2002. **34**(4): p. 563-576.
40. Maro, G.S., M.P. Klassen, and K. Shen, *A β-catenin-dependent Wnt pathway mediates anteroposterior axon guidance in C. elegans motor neurons.* PloS one, 2009. **4**(3): p. e4690.
41. Hartin, S.N., et al., *A Synthetic Lethal Screen Identifies a Role for Lin-44/Wnt in C. elegans Embryogenesis.* 2015.
42. Harterink, M., et al., *Neuroblast migration along the anteroposterior axis of C. elegans is controlled by opposing gradients of Wnts and a secreted Frizzled-related protein.* Development, 2011. **138**(14): p. 2915-2924.
43. Pan, C.-L., et al., *Multiple Wnts and Frizzled Receptors Regulate Anteriorly Directed Cell and Growth Cone Migrations in Caenorhabditis elegans.* Developmental cell, 2006. **10**(3): p. 367-377.
44. Herman, M.A., et al., *The C. elegans gene lin-44, which controls the polarity of certain asymmetric cell divisions, encodes a Wnt protein and acts cell nonautonomously.* Cell, 1995. **83**(1): p. 101-110.
45. Whangbo, J. and C. Kenyon, *A Wnt signaling system that specifies two patterns of cell migration in C. elegans.* Molecular cell, 1999. **4**(5): p. 851-858.
46. Schnorrer, F. and B.J. Dickson, *Axon guidance: morphogens show the way.* Current Biology, 2004. **14**(1): p. R19-R21.
47. Bülow, H.E. and O. Hobert, *Differential sulfations and epimerization define heparan sulfate specificity in nervous system development.* Neuron, 2004. **41**(5): p. 723-736.
48. Inatani, M., et al., *Mammalian brain morphogenesis and midline axon guidance require heparan sulfate.* Science, 2003. **302**(5647): p. 1044-1046.
49. Bornemann, D.J., et al., *Abrogation of heparan sulfate synthesis in Drosophila disrupts the Wingless, Hedgehog and Decapentaplegic signaling pathways.* Development, 2004. **131**(9): p. 1927-1938.
50. Herman, T., E. Hartwieg, and H.R. Horvitz, *sqv mutants of Caenorhabditis elegans are defective in vulval epithelial invagination.* Proceedings of the National Academy of Sciences, 1999. **96**(3): p. 968-973.
51. Morio, H., et al., *EXT gene family member rib-2 is essential for embryonic development and heparan sulfate biosynthesis in Caenorhabditis elegans.*

Biochemical and biophysical research communications, 2003. **301**(2): p. 317-323.
52. Perrimon, N. and M. Bernfield, *Specificities of heparan sulphate proteoglycans in developmental processes.* Nature, 2000. **404**(6779): p. 725-728.
53. Lindahl, U., M. Kusche-Gullberg, and L. Kjellén, *Regulated diversity of heparan sulfate.* Journal of Biological Chemistry, 1998. **273**(39): p. 24979-24982.
54. Krueger, N.X., et al., *Functions of the ectodomain and cytoplasmic tyrosine phosphatase domains of receptor protein tyrosine phosphatase Dlar in vivo.* Molecular and cellular biology, 2003. **23**(19): p. 6909-6921.
55. den Hertog, J., *Protein-tyrosine phosphatases in development.* Mechanisms of development, 1999. **85**(1): p. 3-14.
56. Paul, S. and P. Lombroso, *Receptor and nonreceptor protein tyrosine phosphatases in the nervous system.* Cellular and Molecular Life Sciences CMLS, 2003. **60**(11): p. 2465-2482.
57. Ensslen-Craig, S.E. and S.M. Brady-Kalnay, *Receptor protein tyrosine phosphatases regulate neural development and axon guidance.* Developmental biology, 2004. **275**(1): p. 12-22.
58. Fox, A.N. and K. Zinn, *The heparan sulfate proteoglycan syndecan is an in vivo ligand for the Drosophila LAR receptor tyrosine phosphatase.* Current biology, 2005. **15**(19): p. 1701-1711.
59. Rawson, J.M., et al., *The heparan sulfate proteoglycans Dally-like and Syndecan have distinct functions in axon guidance and visual-system assembly in Drosophila.* Current biology, 2005. **15**(9): p. 833-838.
60. Steigemann, P., et al., *Heparan sulfate proteoglycan syndecan promotes axonal and myotube guidance by slit/robo signaling.* Current biology, 2004. **14**(3): p. 225-230.
61. Wang, F., et al., *LAR receptor tyrosine phosphatases and HSPGs guide peripheral sensory axons to the skin.* Current Biology, 2012. **22**(5): p. 373-382.
62. Lee, J.-S. and C.-B. Chien, *When sugars guide axons: insights from heparan sulphate proteoglycan mutants.* Nature Reviews Genetics, 2004. **5**(12): p. 923-935.
63. Kamath, R.S., et al., *Systematic functional analysis of the Caenorhabditis elegans genome using RNAi.* Nature, 2003. **421**(6920): p. 231-237.
64. Kramer, J.M., *Basement membranes.* 2005.
65. Bernadskaya, Y.Y., et al., *UNC-40/DCC, SAX-3/Robo, and VAB-1/Eph polarize F-actin during embryonic morphogenesis by regulating the WAVE/SCAR actin nucleation complex.* PLoS genetics, 2012. **8**(8): p. e1002863.
66. Mörck, C., et al., *C. elegans ten-1 is synthetic lethal with mutations in cytoskeleton regulators, and enhances many axon guidance defective mutants.* BMC developmental biology, 2010. **10**(1): p. 55.
67. Chen, L., B. Ong, and V. Bennett, *LAD-1, the Caenorhabditis elegans L1CAM homologue, participates in embryonic and gonadal morphogenesis and is a substrate for fibroblast growth factor receptor pathway-dependent phosphotyrosine-based signaling.* The Journal of cell biology, 2001. **154**(4): p. 841-856.

68. Ghenea, S., et al., *The VAB-1 Eph receptor tyrosine kinase and SAX-3/Robo neuronal receptors function together during C. elegans embryonic morphogenesis.* Development, 2005. **132**(16): p. 3679-3690.
69. Morton, D.G., W.A. Hoose, and K.J. Kemphues, *A genome-wide RNAi screen for enhancers of par mutants reveals new contributors to early embryonic polarity in Caenorhabditis elegans.* Genetics, 2012. **192**(3): p. 929-942.
70. Lundquist, E.A. and R.K. Herman, *The mec-8 gene of Caenorhabditis elegans affects muscle and sensory neuron function and interacts with three other genes: unc-52, smu-1 and smu-2.* Genetics, 1994. **138**(1): p. 83-101.
71. Davies, A.G., et al., *Functional overlap between the mec-8 gene and five sym genes in Caenorhabditis elegans.* Genetics, 1999. **153**(1): p. 117-134.
72. van Haaften, G., et al., *Gene interactions in the DNA damage-response pathway identified by genome-wide RNA-interference analysis of synthetic lethality.* Proceedings of the National Academy of Sciences of the United States of America, 2004. **101**(35): p. 12992-12996.
73. Baugh, L.R., et al., *Synthetic lethal analysis of Caenorhabditis elegans posterior embryonic patterning genes identifies conserved genetic interactions.* Genome biology, 2005. **6**(5): p. R45.
74. Mani, K. and D.S. Fay, *A Mechanistic Basis for the Coordinated Regulation of Pharyngeal Morphogenesis in Caenorhabditis elegans by LIN-35/Rb and UBC-18–ARI-1.* PLoS genetics, 2009. **5**(6): p. e1000510.
75. McLellan, J., et al., *Synthetic Lethal Genetic Interactions That Decrease Somatic Cell Proliferation in Caenorhabditis elegans Identify the Alternative RFCCTF18 as a Candidate Cancer Drug Target.* Molecular biology of the cell, 2009. **20**(24): p. 5306-5313.
76. Mohamed, A.M. and I.D. Chin-Sang, *The C. elegans nck-1 gene encodes two isoforms and is required for neuronal guidance.* Developmental biology, 2011. **354**(1): p. 55-66.
77. Pulido, R., et al., *The LAR/PTP delta/PTP sigma subfamily of transmembrane protein-tyrosine-phosphatases: multiple human LAR, PTP delta, and PTP sigma isoforms are expressed in a tissue-specific manner and associate with the LAR-interacting protein LIP. 1.* Proceedings of the National Academy of Sciences, 1995. **92**(25): p. 11686-11690.
78. Sommer, L., M. Rao, and D.J. Anderson, *RPTPd and the Novel Protein Tyrosine Phosphatase RPTPP are Expressed in Restricted Regions of the Developing Central Nervous System.* Developmental dynamics, 1997. **208**(1): p. 48-61.
79. Shen, P., et al., *Expression of a truncated receptor protein tyrosine phosphatase kappa in the brain of an adult transgenic mouse.* Brain research, 1999. **826**(2): p. 157-171.
80. Sun, Q., et al., *Receptor tyrosine phosphatases regulate axon guidance across the midline of the Drosophila embryo.* Development, 2000. **127**(4): p. 801-812.
81. Stoker, A.W., *Receptor tyrosine phosphatases in axon growth and guidance.* Current opinion in neurobiology, 2001. **11**(1): p. 95-102.

82. Sajnani, G., et al., *PTPσ promotes retinal neurite outgrowth non‐cell‐autonomously.* Journal of neurobiology, 2005. **65**(1): p. 59-71.
83. Lee, S., et al., *Dimerization of protein tyrosine phosphatase σ governs both ligand binding and isoform specificity.* Molecular and cellular biology, 2007. **27**(5): p. 1795-1808.
84. Gonzalez-Brito, M.R. and J.L. Bixby, *Protein tyrosine phosphatase receptor type O regulates development and function of the sensory nervous system.* Molecular and Cellular Neuroscience, 2009. **42**(4): p. 458-465.
85. Takahashi, H. and A.M. Craig, *Protein tyrosine phosphatases PTPδ, PTPσ, and LAR: presynaptic hubs for synapse organization.* Trends in neurosciences, 2013. **36**(9): p. 522-534.
86. Schaapveld, R.Q., et al., *Impaired mammary gland development and function in mice lacking LAR receptor-like tyrosine phosphatase activity.* Developmental biology, 1997. **188**(1): p. 134-146.
87. Wang, Z., et al., *Mutational analysis of the tyrosine phosphatome in colorectal cancers.* Science, 2004. **304**(5674): p. 1164-1166.
88. Aricescu, A.R., et al., *Heparan sulfate proteoglycans are ligands for receptor protein tyrosine phosphatase σ.* Molecular and cellular biology, 2002. **22**(6): p. 1881-1892.
89. O'Grady, P., T.C. Thai, and H. Saito, *The laminin–nidogen complex is a ligand for a specific splice isoform of the transmembrane protein tyrosine phosphatase LAR.* The Journal of cell biology, 1998. **141**(7): p. 1675-1684.
90. Coles, C.H., et al., *Proteoglycan-specific molecular switch for RPTPσ clustering and neuronal extension.* Science, 2011. **332**(6028): p. 484-488.
91. Escobedo, N., et al., *Syndecan 4 interacts genetically with Vangl2 to regulate neural tube closure and planar cell polarity.* Development, 2013. **140**(14): p. 3008-3017.
92. Kaksonen, M., et al., *Syndecan-3-deficient mice exhibit enhanced LTP and impaired hippocampus-dependent memory.* Molecular and Cellular Neuroscience, 2002. **21**(1): p. 158-172.
93. Salmivirta, M. and M. Jalkanen, *Syndecan family of cell surface proteoglycans: developmentally regulated receptors for extracellular effector molecules.* Experientia, 1995. **51**(9-10): p. 863-872.
94. Brauker, J.H., M.S. Trautman, and M. Bernfield, *Syndecan, a cell surface proteoglycan, exhibits a molecular polymorphism during lung development.* Developmental biology, 1991. **147**(2): p. 285-292.
95. Chernousov, M.A. and D. Carey, *N-syndecan (syndecan 3) from neonatal rat brain binds basic fibroblast growth factor.* Journal of Biological Chemistry, 1993. **268**(22): p. 16810-16814.
96. Coutts, J.C. and J.T. Gallagher, *Receptors for fibroblast growth factors.* Immunology and cell biology, 1995. **73**(6): p. 584-590.
97. Carmona-Fontaine, C., H. Matthews, and R. Mayor, *Directional cell migration in vivo: Wnt at the crest.* Cell adhesion & migration, 2008. **2**(4): p. 240-242.

98. Dani, N., et al., *A targeted glycan-related gene screen reveals heparan sulfate proteoglycan sulfation regulates WNT and BMP trans-synaptic signaling.* PLoS genetics, 2012. **8**(11): p. e1003031.
99. Minniti, A.N., et al., *Caenorhabditis elegans syndecan (SDN-1) is required for normal egg laying and associates with the nervous system and the vulva.* Journal of cell science, 2004. **117**(21): p. 5179-5190.
100. Lee, J.-Y., et al., *Wnt/Frizzled signaling controls C. elegans gastrulation by activating actomyosin contractility.* Current biology, 2006. **16**(20): p. 1986-1997.
101. Nance, J. and J.R. Priess, *Cell polarity and gastrulation in C. elegans.* Development, 2002. **129**(2): p. 387-397.
102. George, S.E., et al., *The VAB-1 Eph receptor tyrosine kinase functions in neural and epithelial morphogenesis in C. elegans.* Cell, 1998. **92**(5): p. 633-643.
103. Chin-Sang, I.D., et al., *The ephrin VAB-2/EFN-1 functions in neuronal signaling to regulate epidermal morphogenesis in C. elegans.* Cell, 1999. **99**(7): p. 781-790.
104. Li, X., et al., *Somatic gonad sheath cells and Eph receptor signaling promote germ-cell death in C. elegans.* Cell Death & Differentiation, 2012. **19**(6): p. 1080-1089.
105. Gort, E., et al., *The TWIST1 oncogene is a direct target of hypoxia-inducible factor-2α.* Oncogene, 2008. **27**(11): p. 1501-1510.
106. Shao, Z., Y. Zhang, and J.A. Powell-Coffman, *Two distinct roles for EGL-9 in the regulation of HIF-1-mediated gene expression in Caenorhabditis elegans.* Genetics, 2009. **183**(3): p. 821-829.
107. Park, E.C., et al., *Hypoxia regulates glutamate receptor trafficking through an HIF‐independent mechanism.* The EMBO journal, 2012. **31**(6): p. 1379-1393.
108. Ceron, J., et al., *Large-scale RNAi screens identify novel genes that interact with the C. elegans retinoblastoma pathway as well as splicing-related components with synMuv B activity.* BMC developmental biology, 2007. **7**(1): p. 30.
109. Hamamichi, S., et al., *Hypothesis-based RNAi screening identifies neuroprotective genes in a Parkinson's disease model.* Proceedings of the National Academy of Sciences, 2008. **105**(2): p. 728-733.
110. Simmer, F., et al., *Genome-wide RNAi of C. elegans using the hypersensitive rrf-3 strain reveals novel gene functions.* PLoS biology, 2003. **1**(1): p. e12.
111. Tucker, M. and M. Han, *Muscle cell migrations of C. elegans are mediated by the α-integrin INA-1, Eph receptor VAB-1, and a novel peptidase homologue MNP-1.* Developmental biology, 2008. **318**(2): p. 215-223.
112. Costa, M., et al., *A putative catenin–cadherin system mediates morphogenesis of the Caenorhabditis elegans embryo.* The Journal of cell biology, 1998. **141**(1): p. 297-308.
113. Alexander, C.M., et al., *Syndecan-1 is required for Wnt-1-induced mammary tumorigenesis in mice.* Nature genetics, 2000. **25**(3): p. 329-332.
114. Muñoz, R., et al., *Syndecan-4 regulates non-canonical Wnt signalling and is essential for convergent and extension movements in Xenopus embryos.* Nature cell biology, 2006. **8**(5): p. 492-500.

115. Gleason, J.E., E.A. Szyleyko, and D.M. Eisenmann, *Multiple redundant Wnt signaling components function in two processes during C. elegans vulval development.* Developmental biology, 2006. **298**(2): p. 442-457.
116. Sawa, H., L. Lobel, and H.R. Horvitz, *The Caenorhabditis elegans gene lin-17, which is required for certain asymmetric cell divisions, encodes a putative seven-transmembrane protein similar to the Drosophila frizzled protein.* Genes & development, 1996. **10**(17): p. 2189-2197.
117. Hilliard, M.A. and C.I. Bargmann, *Wnt Signals and Frizzled Activity Orient Anterior-Posterior Axon Outgrowth in C. elegans.* Developmental cell, 2006. **10**(3): p. 379-390.
118. Klassen, M.P. and K. Shen, *Wnt signaling positions neuromuscular connectivity by inhibiting synapse formation in C. elegans.* Cell, 2007. **130**(4): p. 704-716.
119. Wu, M. and M.A. Herman, *Asymmetric localizations of LIN-17/Fz and MIG-5/Dsh are involved in the asymmetric B cell division in C. elegans.* Developmental biology, 2007. **303**(2): p. 650-662.
120. Kirszenblat, L., D. Pattabiraman, and M.A. Hilliard, *LIN-44/Wnt directs dendrite outgrowth through LIN-17/Frizzled in C. elegans Neurons.* PLoS biology, 2011. **9**(9): p. e1001157.
121. Brenner, S., *The genetics of Caenorhabditis elegans.* Genetics, 1974. **77**(1): p. 71-94.
122. Schneider, C.A., W.S. Rasband, and K.W. Eliceiri, *NIH Image to ImageJ: 25 years of image analysis.* Nature methods, 2012. **9**(7): p. 671-675.
123. Linkert, M., et al., *Metadata matters: access to image data in the real world.* The Journal of cell biology, 2010. **189**(5): p. 777-782.
124. Hobert, O., K. Tessmar, and G. Ruvkun, *The Caenorhabditis elegans lim-6 LIM homeobox gene regulates neurite outgrowth and function of particular GABAergic neurons.* Development, 1999. **126**(7): p. 1547-1562.
125. Najarro, E.H. and B.D. Ackley, *C. elegans fmi-1/flamingo and Wnt pathway components interact genetically to control the anteroposterior neurite growth of the VD GABAergic neurons.* Developmental biology, 2013. **377**(1): p. 224-235.
126. Shen, Y., *Traffic lights for axon growth: proteoglycans and their neuronal receptors.* Neural Regeneration Research, 2014. **9**(4): p. 356.
127. Bülow, H.E., et al., *Extracellular sugar modifications provide instructive and cell-specific information for axon-guidance choices.* Current Biology, 2008. **18**(24): p. 1978-1985.
128. Van Vactor, D., D.P. Wall, and K.G. Johnson, *Heparan sulfate proteoglycans and the emergence of neuronal connectivity.* Current opinion in neurobiology, 2006. **16**(1): p. 40-51.
129. Yamaguchi, Y. *Heparan sulfate proteoglycans in the nervous system: their diverse roles in neurogenesis, axon guidance, and synaptogenesis*. in *Seminars in cell & developmental biology*. 2001. Elsevier.
130. Bernfield, M., et al., *Biology of the syndecans: a family of transmembrane heparan sulfate proteoglycans.* Annual review of cell biology, 1992. **8**(1): p. 365-393.

131. Wang, X., et al., *The heparan sulfate-modifying enzyme glucuronyl C5-epimerase HSE-5 Controls C. elegans Q neuroblast polarization during migration.* Developmental Biology, 2015.
132. Tumova, S., A. Woods, and J.R. Couchman, *Heparan sulfate proteoglycans on the cell surface: versatile coordinators of cellular functions.* The international journal of biochemistry & cell biology, 2000. **32**(3): p. 269-288.
133. Baeg, G.-H. and N. Perrimon, *Functional binding of secreted molecules to heparan sulfate proteoglycans in Drosophila.* Current opinion in cell biology, 2000. **12**(5): p. 575-580.
134. Hsueh, Y.-P. and M. Sheng, *Regulated expression and subcellular localization of syndecan heparan sulfate proteoglycans and the syndecan-binding protein CASK/LIN-2 during rat brain development.* The Journal of neuroscience, 1999. **19**(17): p. 7415-7425.
135. Forrester, W.C., C. Kim, and G. Garriga, *The Caenorhabditis elegans Ror RTK CAM-1 inhibits EGL-20/Wnt signaling in cell migration.* Genetics, 2004. **168**(4): p. 1951-1962.
136. Green, J.L., T. Inoue, and P.W. Sternberg, *The C. elegans ROR receptor tyrosine kinase, CAM-1, non-autonomously inhibits the Wnt pathway.* Development, 2007. **134**(22): p. 4053-4062.
137. Forrester, W.C., et al., *A C. elegans Ror receptor tyrosine kinase regulates cell motility and asymmetric cell division.* Nature, 1999. **400**(6747): p. 881-885.
138. Kennerdell, J.R., R.D. Fetter, and C.I. Bargmann, *Wnt-Ror signaling to SIA and SIB neurons directs anterior axon guidance and nerve ring placement in C. elegans.* Development, 2009. **136**(22): p. 3801-3810.
139. Hayashi, Y., et al., *A trophic role for Wnt-Ror kinase signaling during developmental pruning in Caenorhabditis elegans.* Nature neuroscience, 2009. **12**(8): p. 981-987.
140. Minami, Y., et al., *Ror‐family receptor tyrosine kinases in noncanonical Wnt signaling: Their implications in developmental morphogenesis and human diseases.* Developmental Dynamics, 2010. **239**(1): p. 1-15.
141. Song, S., et al., *A Wnt-Frz/Ror-Dsh pathway regulates neurite outgrowth in Caenorhabditis elegans.* PLoS genetics, 2010. **6**(8): p. e1001056.
142. Grill, B., et al., *C. elegans RPM-1 regulates axon termination and synaptogenesis through the Rab GEF GLO-4 and the Rab GTPase GLO-1.* Neuron, 2007. **55**(4): p. 587-601.
143. Thompson, O., et al., *The million mutation project: a new approach to genetics in Caenorhabditis elegans.* Genome research, 2013. **23**(10): p. 1749-1762.
144. Buechling, T. and M. Boutros, *2 Wnt Signaling: Signaling at and Above the Receptor Level.* Current topics in developmental biology, 2011. **97**: p. 21.
145. Bernfield, M., et al., *Functions of cell surface heparan sulfate proteoglycans.* Annual review of biochemistry, 1999. **68**(1): p. 729-777.
146. Kinnunen, T.K., *Combinatorial Roles of Heparan Sulfate Proteoglycans and Heparan Sulfates in Caenorhabditis elegans Neural Development.* PloS one, 2014. **9**(7): p. e102919.

147. Baker, S.T., et al., *RPM-1 uses both ubiquitin ligase and phosphatase-based mechanisms to regulate DLK-1 during neuronal development.* PLoS genetics, 2014. **10**(5): p. e1004297.